European Journal of Medicinal Chemistry 213 (2021) 113215

Contents lists available at ScienceDirect

European Journal of Medicinal Chemistry

journal homepage: http://www.elsevier.com/locate/ejmech

Research paper

Discovery of novel 4-azaaryl-*N*-phenylpyrimidin-2-amine derivatives as potent and selective FLT3 inhibitors for acute myeloid leukaemia with *FLT3* mutations

Yi Long, Mingfeng Yu, Aleksandra M. Ochnik, Jasmine D. Karanjia, Sunita KC. Basnet, Alemwork A. Kebede, Lianmeng Kou, Shudong Wang*

Drug Discovery and Development, Clinical and Health Sciences, University of South Australia, Adelaide, SA, 5001, Australia

ARTICLE INFO

Article history:
Received 6 December 2020
Received in revised form
15 January 2021
Accepted 15 January 2021
Available online 22 January 2021

Keywords:
AML
FLT3 inhibitor
FLT3-ITD
FLT3-D835Y
Anti-AML drug discovery

ABSTRACT

Feline McDonough sarcoma (FMS)-like tyrosine kinase 3 (FLT3) is one of the most pursued targets in the treatment of acute myeloid leukaemia (AML) as its gene amplification and mutations, particularly internal tandem duplication (ITD), contribute to the pathogenesis of AML and the resistance to known FLT3 inhibitors. To conquer this challenge, there is a quest for structurally novel FLT3 inhibitors. Herein, we report the discovery of a new series of 4-azaaryl-*N*-phenylpyrimidin-2-amine derivatives as potent and selective FLT3 inhibitors. Compounds **12b** and **12r** were capable of suppressing a wide range of mutated FLT3 kinases including ITD and D835Y mutants; the latter isoform is closely associated with acquired drug resistance. In addition, both compounds displayed an anti-proliferative specificity for *FLT3*-ITD-harbouring cell lines (*i.e.*, MV4-11 and MOLM-13 cells) over those with expression of the wild-type kinase or even without FLT3 expression. In mechanistic studies using MV4-11 cells, **12b** was found to diminish the phosphorylation of key downstream effectors of FLT3 and induce apoptosis, supporting an FLT3-ITD-targeted mechanism of its anti-proliferative action.

1. Introduction

Acute myeloid leukaemia (AML) is an aggressive haematopoietic malignancy originating from abnormal proliferation of myeloid progenitor cells within the blood circulation and bone marrow, and is associated with a poor prognosis and a sluggish response to chemotherapy [1–3]. The clinical prognosis is contingent on patient age, exposure to upfront chemotherapy, performance status, and genetic profile including the occurrence of mutations in the *feline McDonough sarcoma (FMS)-like tyrosine kinase 3* (*FLT3*) gene [4,5], with survival rates being 60–70% in paediatric patients and lower than half in adult patients [6].

FLT3 is a member of the class III subfamily of receptor tyrosine kinases, and is primarily expressed in the haematopoietic system (*e.g.*, immature myeloid and lymphoid progenitors), while its ligand is present in a number of tissues such as liver, thymus, spleen, placenta, heart, lung and so forth [2,7–9]. Inactive FLT3 exists as an unphosphorylated monomer, and is stimulated upon binding to its ligand and undergoes a conformational transformation that facilitates receptor-receptor dimerisation and activation of its intrinsic tyrosine kinase activity [10,11]. Subsequently, activated FLT3 autophosphorylates multiple sites in the intracellular domain, promoting the recruitment of various proteins and giving rise to a series of sophisticated protein-protein interactions [12]. The protein complex thus assembled initiates the cascades of phosphorylation reactions among diverse intracellular kinases and enables the activation of their associated signalling pathways (*e.g.*, RAS/RAF/MEK/ERK, JAK/STAT5 and PI3K/AKT/mTOR), thereby regulating differentiation, proliferation and survival of normal haematopoietic cells [2,10,13–15].

However, genetic alterations of the *FLT3* gene, mainly comprising internal tandem duplications (ITDs) in the juxtamembrane domain and point mutations in the tyrosine kinase domain, have been identified in approximately one third of AML patients, and are among the most prevalent genetic abnormalities occurring in AML [16,17]. These *FLT3* mutations confer ligand-independent, constitutive activation of downstream signalling pathways and subsequently induce aberrant proliferation of AML cells, leading to

* Corresponding author.
E-mail address: shudong.wang@unisa.edu.au (S. Wang).

https://doi.org/10.1016/j.ejmech.2021.113215
0223-5234/

a higher relapse rate and an inferior overall survival in AML patients [4,18,19]. The same holds true for the cases with overexpression of wild-type (WT) FLT3 receptors yet in the absence of *FLT3*-ITD [20]. Therefore, FLT3 and its common mutant forms have been regarded as legitimate molecular therapeutic targets for the treatment of AML.

An arsenal of FLT3 inhibitors with various degrees of inhibitory potency and selectivity have been developed (Fig. 1) [4,21]. The initial wave of FLT3 inhibitors were co-opted from the molecules originally designed to target alternative kinases, and therefore are non-specific towards FLT3 [17,22,23]. Well-studied inhibitors of this generation include sunitinib, sorafenib, midostaurin and lestaurtinib. Despite their high potency against FLT3 *in vitro*, most of these inhibitors have toxicity issues and limited efficacy, and thus generally failed in early-phase clinical trials where they had been used as single agents in relapsed or refractory AML patients [2,10,17,22,24,25]. Accordingly, newer-generation FLT3 inhibitors with enhanced selectivity have emerged; typical examples are quizartinib, crenolanib, gilteritinib and pexidartinib. These inhibitors were found generally well-tolerated in phase I/II clinical trials [17,24], but their inhibition of multiple other kinases and suboptimal pharmacokinetics remain severe disadvantages. Among both generations of FLT3 inhibitors, midostaurin and gilteritinib were approved by the USFDA for the treatment of *FLT3*-mutated AML in 2017 and 2018, respectively, whereas quizartinib received Japanese regulatory approval for its use in *FLT3*-ITD-positive patients last year. Nevertheless, the clinical success of other FLT3 inhibitors under development is mostly hampered by partial and transient clinical responses, adverse events as well as unfavourable pharmacokinetics. These roadblocks might be overcome, for example, by the discovery and development of FLT3 inhibitors with new pharmacophores.

In our previous tremendous attempts to identify novel, potent and selective inhibitors of individual CDKs [26–32], a few of the compounds with little CDK inhibitory activity unexpectedly exerted potent anti-proliferative effects on MV4-11 AML cells. This intriguing phenomenon has urged us to explore their *bona fide* kinase targets, and one of such interesting compounds was **12b** with an *N*-phenylpyrimidin-2-amine scaffold (Fig. 2). Herein, we report the identification of **12b** as an FLT3 inhibitor, molecular-docking-guided structural modification of this compound, and cellular mechanistic investigation of **12b** and its analogue **12r**.

2. Results and discussion

2.1. Identification of *12b* as an FLT3 inhibitor

As briefly aforementioned, compound **12b** was inactive towards CDKs (K_i > 5 μM), but displayed potent anti-proliferative activity against MV4-11 AML cells with a GI_{50} value of 0.074 μM (Fig. 2). To identify its genuine kinase targets, this compound was further assessed against a panel of 44 non-CDK kinases at a concentration

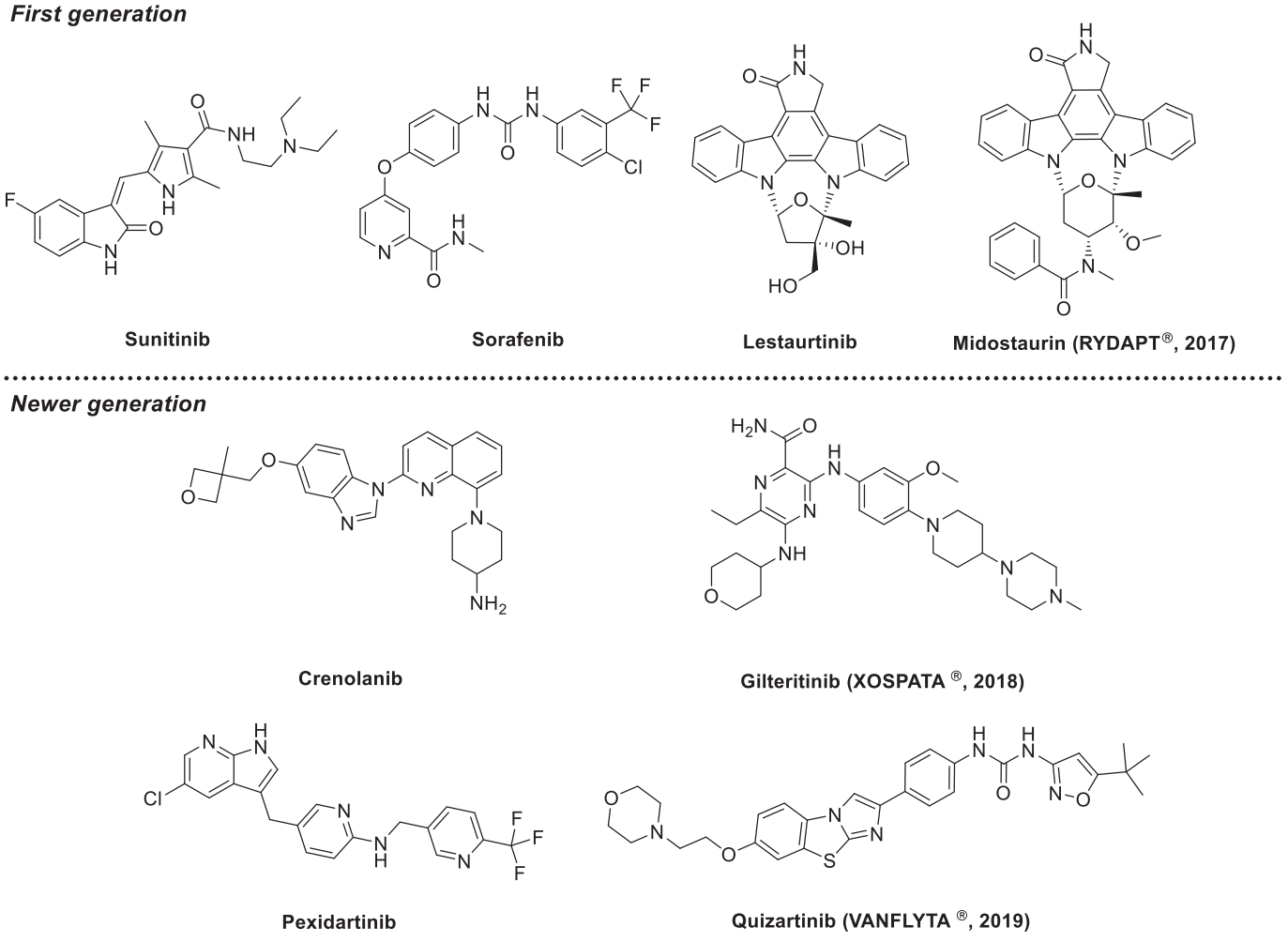

Fig. 1. Chemical structures of selected FLT3 inhibitors.

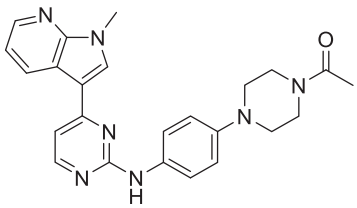

Kinase inhibition, K_i (μM)			72 h growth inhibition, GI_{50} (μM)
CDKs 1-7 & 9	FLT3-WT	FLT3-ITD	MV4-11
> 5	0.009	0.002	0.074 ± 0.010

Fig. 2. Chemical structure and biological activity of **12b**.

of 1 μM, revealing that: (i) **12b** potently inhibited FLT3 and its ITD mutant with inhibition being > 90%; and (ii) the majority of the other kinases tested were not, or only slightly, suppressed (*i.e.*, < 50% inhibition) (Fig. 3). Later, K_i values of **12b** for FLT3-WT and -ITD were determined to be 0.009 and 0.002 μM, respectively (Fig. 2). These enzymatic data indicate that **12b** is a potent inhibitor of FLT3 with a reasonable degree of selectivity.

To probe the molecular basis for the potent FLT3 inhibitory activity of **12b**, this compound was docked into the crystal structure of FLT3 (PDB ID: 4RT7) using Glide (Schrödinger Inc., 2013) (Fig. 4A), and the binding mode thus obtained was compared to that of the quizartinib-FLT3 co-crystal structure (PDB ID: 4RT7) (Fig. 4B). Compound **12b** is predicted to bind to FLT3 through interactions of different nature (Fig. 4A). Specifically, pyrimidinyl-N3 of **12b** forms a bifurcated hydrogen bond with both the ε-ammonium group (NH_3^+) of Lys644 and the backbone NH of Asp829 from the DFG motif, while the bridging secondary amino and terminal acetyl groups generate a total of two hydrogen bonds with the backbone carbonyl of Asp829 and the backbone NH of the hinge residue Cys694, respectively. The phenyl ring of **12b** is sandwiched between the gatekeeper residue Phe691 and DFG-Phe830, forming π-π stacking that likely reinforces the stabilisation of **12b**-FLT3 binding. In addition, the pyrrolo[2,3-*b*]pyridin-3-yl moiety extends into the back cleft [33] of the ATP-binding pocket and hydrophobically interacts with multiple residues including Met664, Met665, Leu802, Cys807 and Val808 (not shown in Fig. 4A). All of these binding features are also seen in the co-crystal structure of quizartinib in complex with FLT3 (Fig. 4B) despite the disparate chemical structures of the two inhibitors, implying that: (i) **12b** might interact with the kinase in a similar manner to quizartinib,

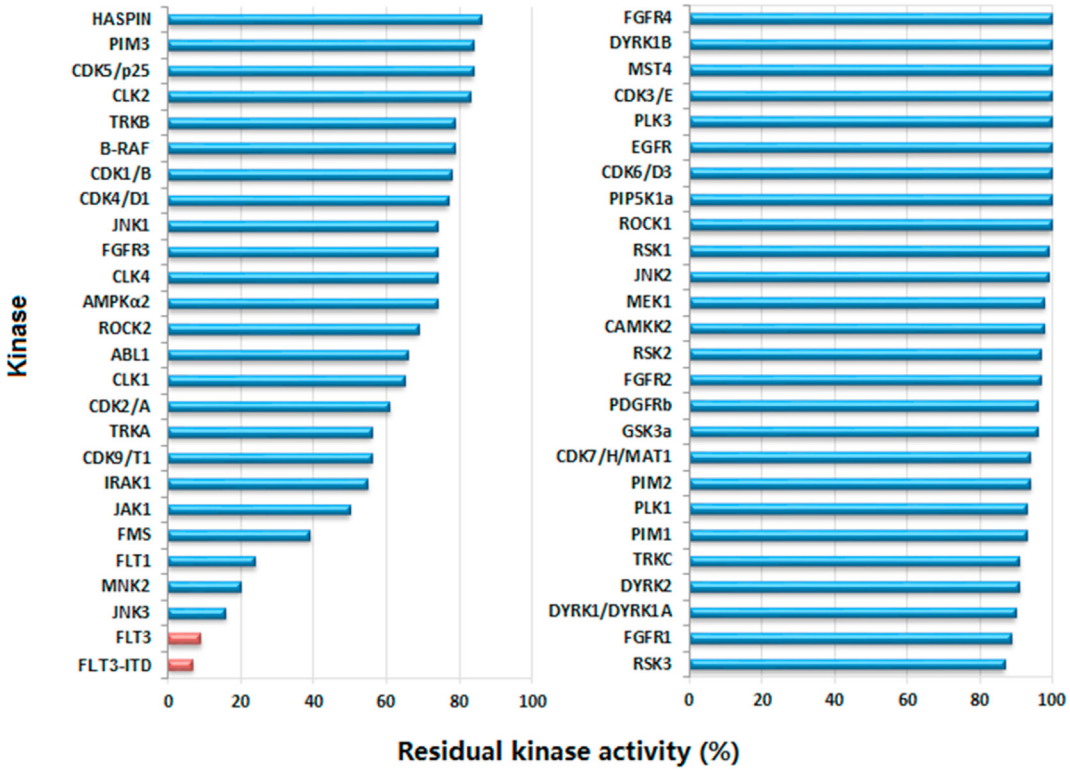

Fig. 3. Kinase selectivity profile of **12b** over a panel of 52 kinases (8 CDKs and 44 non-CDK kinases). Assays were conducted in duplicate at a compound concentration of 1 μM by Reaction Biology Corporation, and the average percentages of residual kinase activity are illustrated.

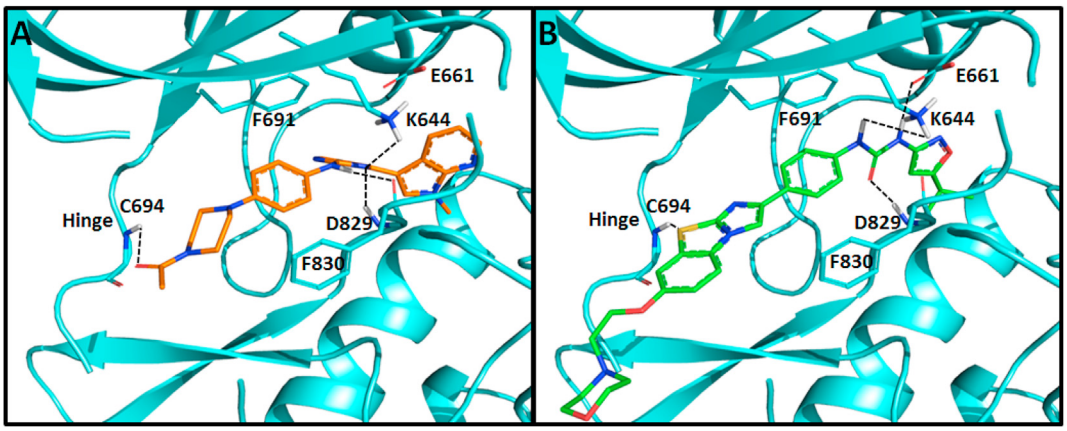

Fig. 4. (**A**) Predicted **12b**-FLT3 binding mode generated using Glide (Schrödinger Inc., 2013), and (**B**) the co-crystal structure of quizartinib in complex with FLT3 (PDB ID: 4RT7). Hydrogen bonds are drawn as black dotted lines and selected residues of FLT3 annotated. The figures were generated using PyMOL 1.7.

and (ii) it would be practical to derive novel FLT3 inhibitors from the structural alteration of **12b** with the aim of improving inhibitory potency and specificity.

2.2. Rational design of *12b* analogues

Given its decent FLT3 inhibitory profile, compound **12b** was considered as a starting point to develop a series of novel analogues as more potent and selective FLT3 inhibitors. The **12b**-FLT3 binding pose generated from the above docking experiment suggested the significance of the *N*-phenylpyrimidin-2-amine scaffold for the inhibition of this kinase (Fig. 4A). Hence, this scaffold was retained. Comparison between the predicted **12b**-FLT3 binding mode and the co-crystal structure of the quizartinib-FLT3 complex revealed that (i) the back cleft of the ATP-binding pocket might be able to accommodate large-size aromatic groups, and (ii) the rigidity could not be required for the hinge-binding moieties. As such, the structural modification of **12b** focused on the diversification of the substituents on the pyrimidinyl-C4 position and the phenyl ring. Specifically, a variety of fused azabiaryl ring systems, including 1*H*-indol-3-yl, 1*H*-indazol-3-yl, 1*H*-pyrrolo[2,3-*b*]pyridin-3-yl and 1*H*-pyrrolo[3,2-*b*]pyridin-3-yl, were introduced onto the C4 position of the central pyrimidine ring on the one hand, and the position and nature of aliphatic azacycles on the phenyl ring, *i.e.*, *p*-(4-acetylpiperazin-1-yl), *m*-(4-methylpiperazin-1-yl) and *m*-(4-acetyl-1,4-diazepan-1-yl), were varied on the other hand. The preparation and biological evaluation of these rationally designed molecules are described below.

2.3. Chemistry

The synthetic route deployed to prepare 4-azaaryl-*N*-phenylpyrimidin-2-amine derivatives **12a**-**12s** is illustrated in Schemes 1 and 2. Acetylation of indoles **1** or azaindoles **3** at their respective C3 positions was effected with cyanoacetic acid or acetyl chloride, respectively, with the yields ranging from 77 to 92% (Scheme 1). While 3-acetylindole **2c** was masked with a toluenesulfonyl (Ts) group to afford **2d** in near-quantitative yield, 3-acetyl-7-azaindole **4b** was further methylated with *N*,*N*-dimethylformamide dimethyl acetal (DMF-DMA) to give **4c** and **4d** in a yield of 51% and 26%, respectively. On the other hand, starting from 1*H*-indazole-3-carboxylic acid **5**, the corresponding carboxamide **6a** and its Boc-protected form **6b** were prepared in 85% and 98% yields, and were subsequently converted into their respective ketones **7a** (95%) and **7b** (81%) using a metal-based reagent. All of ketones **2**, **4** and **7** reacted with either DMF-DMA or 1-*tert*-butoxy-*N*,*N*,*N*′,*N*′-tetramethylmethanediamine (Bredereck's reagent) to afford a variety of enaminones **8** in good to excellent yields. In parallel, the other building blocks—guanidines **11**—were either commercially purchased or modularly synthesised *via* high-yielding guanidinylation of arylamines **10** with aqueous cyanamide, following quantitative palladium-catalysed reduction of the corresponding aryl nitro compounds **9** with gaseous hydrogen (Scheme 2). Ring closure of an enaminone **8** with a guanidine **11** under microwave irradiation eventually gave the desired 4-azaaryl-*N*-phenylpyrimidin-2-amines **12a-12s** in various yields.

2.4. Structure-activity relationships

All compounds were evaluated for their activity against both FLT3-WT and -ITD. Owing to the wide application of their common scaffold, *i.e.*, *N*-phenylpyrimidin-2-amine, in engineering CDK inhibitors, compounds **12a**-**12s** were additionally evaluated for their potency against CDKs 1, 2 and 7 to initially define some off-targets. MV4-11 cells harbour a homozygous *FLT3*-ITD mutation, and their proliferation is known to be FLT3-dependent [34–37]. As a result, this AML cell line was chosen to measure the *in vitro* antiproliferative effects of the compounds. Clinical FLT3 inhibitor gilteritinib served as a positive control, and all the kinase inhibition as well as cell viability data are summarised in Tables 1 and 2.

Structural modification of **12b** ($R^1 = CH_3$) started with unmasking the NH site of the 1*H*-pyrrolo[2,3-*b*]pyridin-3-yl moiety; removal of the methyl group afforded **12a** ($R^1 = H$) with improved inhibitory activity against FLT3-WT ($K_i = 0.0008$ μM), FLT3-ITD ($K_i = 0.0001$ μM) and MV4-11 cells ($GI_{50} < 0.001$ μM) but with a diminished selectivity for FLT3 over CDKs (Table 1). The same phenomenon was also observed for **12c** ($R^1 = H$) and its methyl counterpart **12d** ($R^1 = CH_3$), both of which contain a 4-methylpiperazin-1-yl pendant at the *meta* position of the phenyl ring [*i.e.*, $R^4 = m$-(4-methylpiperazin-1-yl)], as well as for the pair of compounds **12e** (X = N, $R^1 = H$) and **12f** (X = NCH_3, no R^1 substituent) with a larger terminal aliphatic azacycle, *i.e.*, *m*-(4-acetyl-1,4-diazepan-1-yl). Moving the nitrogen atom of **12a**, **12c** and **12e** from the X to Y position gave rise to **12g**, **12h** and **12i**, respectively, which were much less effective inhibitors of FLT3 kinases (K_i: 0.0001–0.004 μM *vs.* 0.004–0.217 μM), CDKs (K_i: 0.029–0.531 μM *vs.* > 5 μM) and MV4-11 cells (GI_{50}: ≤ 0.020 μM *vs.* 0.405–0.688 μM). A close examination of the impact of the R^4 group on FLT3 inhibitory activity (**12a** *vs.* **12c** and **12e**; **12b** *vs.* **12d**; **12g** *vs.* **12h** and **12i**) disclosed that *para*-substitution of the phenyl

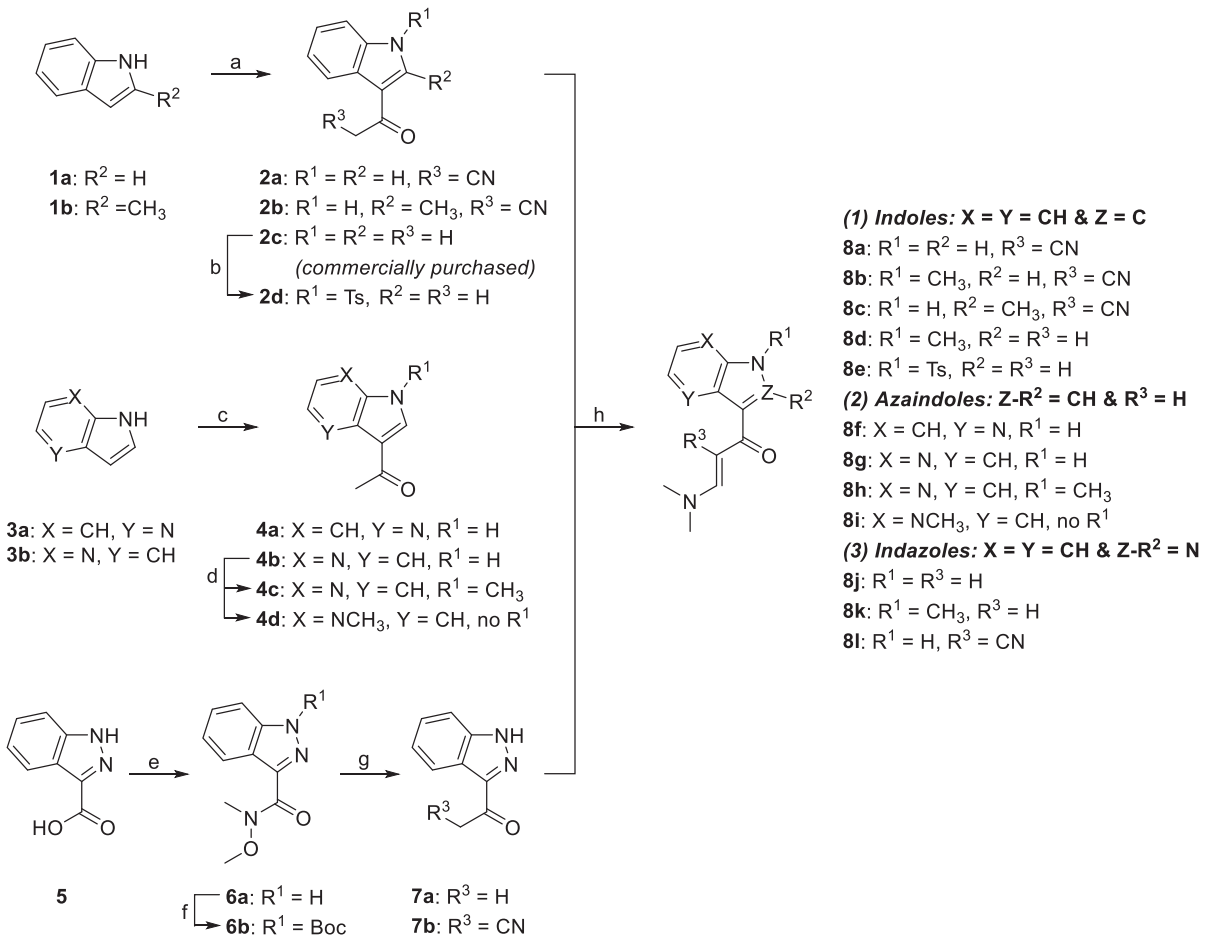

Scheme 1. Synthesis of enaminones **8a**-**8l**. *Reagents and conditions*: (a) cyanoacetic acid, acetic anhydride, 85 °C, 10 min, **2a**: 90% and **2b**: 92%; (b) 4-toluenesulfonyl chloride, tetrabutylammonium hydrogen sulfate, 50% (w/v) aqueous NaOH, DCM, rt, o/n, 99%; (c) acetyl chloride, $AlCl_3$, DCM, rt, o/n, **4a**: 82% and **4b**: 77%; (d) DMF-DMA, reflux, o/n, **4c**: 51% and **4d**: 26%; (e) *N*,*O*-dimethylhydroxylamine hydrochloride, pyridine, EDC·HCl, THF, 0 °C to rt, o/n, 85%; (f) Boc_2O, DMAP, Et_3N, DCM, 0 °C to rt, o/n, 98%; (g) **6a** − CH_3MgBr, THF, −78 °C to rt, 3.5 h, **7a**: 95%; **6b** − CH_3CN, $LiN(iPr)_2$, THF, −78 °C to rt, o/n, **7b**: 81%; (h) DMF-DMA, (1) rt, 5−30 min, (2) reflux, 2−36 h, or (3) microwave 150−300 W, 180 °C, 1 h, 70−98%; or 1-*tert*-butoxy-*N*,*N*,*N*′,*N*′-tetramethylmethanediamine, reflux, 6 h, 69−90%.

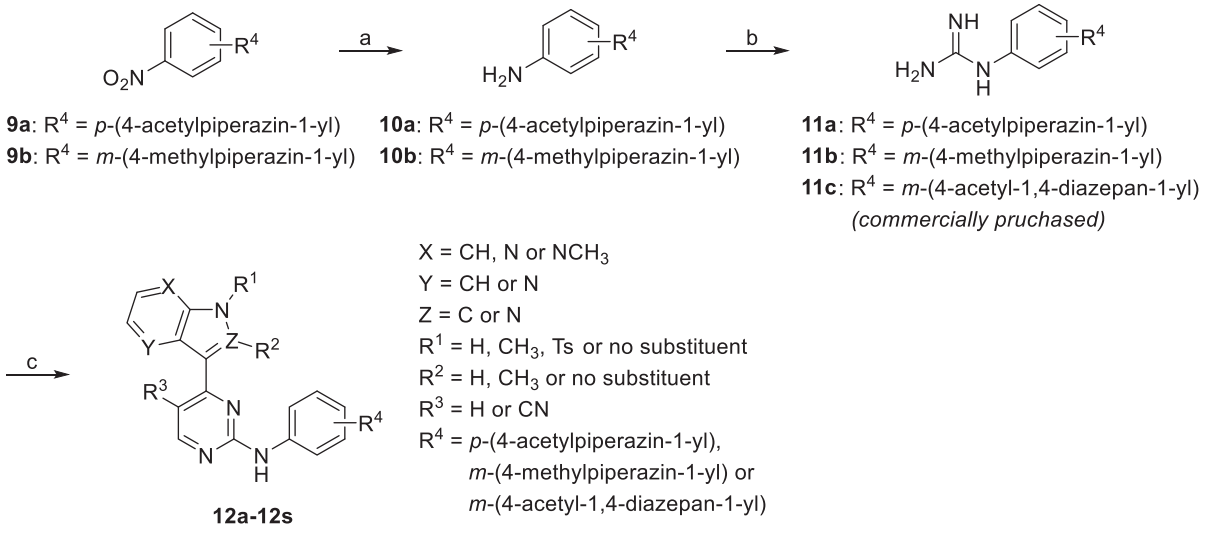

Scheme 2. Synthesis of 4-azaaryl-*N*-phenylpyrimidin-2-amine derivatives **12a**-**12s**. *Reagents and conditions*: (a) H_2, 10% Pd/C, CH_3OH, rt, o/n, **10a**: 100% and **10b**: 100%; (b) H_2NCN, $(CH_3)_3SiCl$, CH_3CN, 0 °C to reflux, o/n, **11a**: 85% and **11b**: 95%; (c) appropriate enaminone **8**, NaOH, 2-methoxyethanol or CH_3CN, microwave 150−300 W, 160 °C, 1 h, 13−64%.

Table 1
Structure and biological activities of **12a**-**12i**.

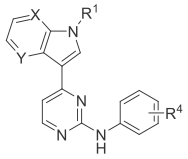

Compound	Structure				Kinase inhibition, K_i (μM)[a]					Growth inhibition, GI_{50} (μM)[b]
	X	Y	R^1	R^4	FLT3-WT	FLT3-ITD	CDK1B	CDK2A	CDK7H	MV4-11
12a	N	CH	H	*p*-(4-acetylpiperazin-1-yl)	0.0008	0.0001	0.091	0.049	>5	<0.001
12b	N	CH	CH_3	*p*-(4-acetylpiperazin-1-yl)	0.009	0.002	>5	>5	>5	0.074 ± 0.010
12c	N	CH	H	*m*-(4-methylpiperazin-1-yl)	0.004	0.002	0.531	0.084	0.142	0.005 ± 0.004
12d	N	CH	CH_3	*m*-(4-methylpiperazin-1-yl)	0.040	0.013	>5	0.970	>5	0.024 ± 0.012
12e	N	CH	H	*m*-(4-acetyl-1,4-diazepan-1-yl)	0.0004	0.0001	0.051	0.031	0.029	0.020 ± 0.003
12f	NCH_3	CH	–	*m*-(4-acetyl-1,4-diazepan-1-yl)	0.001	0.0007	1.756	>5	>5	0.024 ± 0.002
12g	CH	N	H	*p*-(4-acetylpiperazin-1-yl)	0.032	0.004	>5	>5	>5	0.420 ± 0.035
12h	CH	N	H	*m*-(4-methylpiperazin-1-yl)	0.217	0.020	>5	>5	>5	0.405 ± 0.177
12i	CH	N	H	*m*-(4-acetyl-1,4-diazepan-1-yl)	0.150	0.107	>5	>5	>5	0.688 ± 0.041
gilteritinib				–	0.010	0.002	>5	1.485	>5	0.002 ± 0.000

[a] Apparent inhibition constants (K_i) were determined either by Reaction Biology Corporation or using in-house kinase assays; K_i values were calculated using the half maximal inhibition (IC_{50}) and the appropriate K_m(ATP) of each kinase. [b] Anti-proliferative activity was determined using 72 h resazurin assays, and the data given are mean values derived from at least two replicates ± SD.

Table 2
Structure and biological activities of **12j**-**12s**.

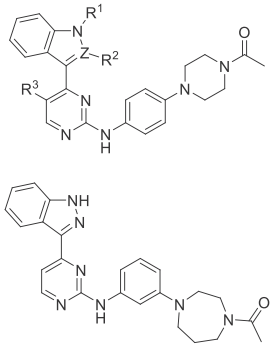

Compound	Structure				Kinase inhibition, K_i (μM)[a]					Growth inhibition, GI_{50} (μM)[b]
	Z	R^1	R^2	R^3	FLT3-WT	FLT3-ITD	CDK1B	CDK2A	CDK7H	MV4-11
12j	C	H	H	H	0.022	0.011	>5	>5	>5	0.033 ± 0.021
12k	C	CH_3	H	H	0.149	0.133	>5	>5	>5	0.252 ± 0.103
12l	C	Ts	H	H	>5	0.128	>5	>5	>5	1.559 ± 0.675
12m	C	H	H	CN	0.004	0.0004	4.055	>5	0.426	0.004 ± 0.001
12n	C	CH_3	H	CN	0.037	0.007	1.581	1.120	1.625	0.030 ± 0.006
12o	C	H	CH_3	CN	0.119	0.002	>5	2.170	0.536	0.390 ± 0.496
12p	N	H	–	H	>5	0.207	>5	>5	>5	0.346 ± 0.130
12q	N	CH_3	–	H	0.883	0.274	>5	>5	>5	0.181 ± 0.054
12r	N	H	–	CN	0.021	0.0002	1.654	>5	>5	0.017 ± 0.012
12s			–		0.001	0.0006	0.727	>5	>5	0.018 ± 0.002
gilteritinib			–		0.010	0.002	>5	1.485	>5	0.002 ± 0.000

[a] Apparent inhibition constants (K_i) were determined either by Reaction Biology Corporation or using in-house kinase assays; K_i values were calculated using the half maximal inhibition (IC_{50}) and the appropriate K_m(ATP) of each kinase. [b] Anti-proliferative activity was determined using 72 h resazurin assays, and the data given are mean values derived from at least two replicates ± SD.

ring with 4-acetylpiperazin-1-yl offered the most potent FLT3 inhibitors, so this substituent remained unchanged during the further variation of the fused azabiaryl ring system at the pyrimidinyl-C4 position, with the single exception of **12s** (Table 2).

Replacement of the 1*H*-pyrrolo[2,3-*b*]pyridin-3-yl headgroup of **12a** and **12b** (X = N, Y = Z = CH) with the 1*H*-indazol-3-yl moiety [*i.e.*, **12p** and **12q** (X = Y= CH, Z = N)] drastically decreased enzymatic and cellular potencies, with K_i values for FLT3-WT and -ITD being greater than 0.2 μM (Tables 1 and 2). However, either introduction of a cyanide group at the pyrimidinyl-C5 position [*i.e.*, **12r** (R^3 = CN)] or substitution of *m*-(4-acetyl-1,4-diazepan-1-yl) for *p*-(4-acetylpiperazin-1-yl) on the terminal phenyl ring (*i.e.*, **12s**) restored the inhibitory activity against FLT3 kinases (K_i = 0.0002–0.021 μM) and MV4-11 cells (GI_{50} = 0.017–0.018 μM)

(Table 2). The former tactic was also deployed to ameliorate the inhibitory effect of the 1*H*-indol-3-yl-headed compounds (X = Y = Z = CH) on both FLT3 kinases and MV4-11 cells. As expected, cyano compounds **12m** (R^1 = H, R^3 = CN) and **12n** (R^1 = CH_3, R^3 = CN) more potently suppressed the activity of the kinases and the proliferation of MV4-11 cells than did their respective non-substituted counterparts **12j** (R^1 = H, R^3 = H) and **12k** (R^1 = CH_3, R^3 = H). Alternative elaborations of the 1*H*-indol-3-yl moiety included (1) masking of the NH site with a bulky tosyl group [*i.e.*,**12j** (R^1 = H) *vs.* **12l** (R^1 = Ts)] and (2) relocation of the methyl group from the indolyl-N1 to -C2 position in the presence of a cyanide group [*i.e.*,**12n** (R^1 = CH_3, R^2 = H, R^3 = CN) *vs.* **12o** (R^1 = H, R^2 = CH_3, R^3 = CN)]. Both strategies were found to be generally detrimental to inhibition of both FLT3 kinases and MV4-11 cells, with the effect being much more profound in the former structural modification.

To sum up, the majority of the compounds are not only single-digit nanomolar or even sub-nanomolar FLT3 inhibitors with decent degrees of selectivity over CDKs, but also effective anti-proliferative agents of MV4-11 cells. Such potencies are comparable, if not superior, to those of gilteritinib. While 1*H*-pyrrolo[2,3-*b*] pyridin-3-yl is the most favourable headgroup in terms of FLT3 inhibitory activity and anti-proliferative effect on MV4-11 cells, installation of a cyanide group at the pyrimidinyl-C5 position (*i.e.*, R^3 = CN) in the context of the 1*H*-ind(az)ol-3-yl-headed compounds generally boosts both enzymatic and cellular potencies.

2.5. Further characterisation of *12b* and *12r*

In addition to *FLT3*-ITD, there are other mutations that occur in AML patients and are highly correlated with a poor prognosis [19]. Consequently, a range of FLT3 mutants were selected to define the scope of the inhibitory activity of the hit compound **12b** and its analogue **12r** (one of the most potent and selective inhibitor of FLT3-ITD). As presented in Table 3, **12r** is far more active than **12b** against every single FLT3 mutant tested. While **12r** is a sub-nanomolar inhibitor of all eight FLT3-mutated isoforms (*i.e.*, K_i < 0.0003 μM), K_i values of **12b** range from 0.002 to 0.262 μM. However, the latter shows a degree of specificity for FLT3-ITD (K_i = 0.002 μM) over the other mutants (K_i = 0.047–0.262 μM). Notably, both **12b** and **12r** are potent inhibitors of FLT3-D835Y—a mutant implicated in acquired clinical resistance to known FLT3 inhibitors [22,38,39], and therefore hold promise to overcome this challenge.

As shown in Tables 1–3, both **12b** and **12r** effectively suppressed the kinase activity of both WT FLT3 and its mutants, particularly, FLT3-ITD, in non-cell-based biochemical assays. To investigate whether such effects could be translated into the anti-proliferative potencies in cell viability assays, the two compounds were screened against a panel of seven leukaemic cell lines with different FLT3 statuses (Table 4). AML cell lines MV4-11 and MOLM-13 carry ITD mutation; THP1 and U937, the other two AML cell lines tested, together with NB4 acute promyelocytic leukaemia cells harbour unmutated *FLT3* gene; no FLT3 is expressed in Jurkat T-cell leukaemia and K562 chronic myeloid leukaemia cell lines [37]. As expected, FLT3-ITD-expressing cells, *i.e.*, MV4-11 and MOLM-13, were very sensitive to compounds **12b** and **12r** (GI_{50} = 0.0004–0.074 μM), whereas the viability of the cells with low or no expression of FLT3 (*i.e.*, U937, Jurkat and K562) was not affected by either inhibitor (GI_{50} > 10 μM). The single exception of the latter case was the moderate anti-proliferative activity of **12r** towards K562 cells (GI_{50} = 0.185 μM), suggesting that the compound might target alternative kinase(s) pivotal for the growth and survival of this cell line. NB4 and THP1 cells with expression of WT FLT3 were inhibited weakly by **12b** or **12r**. Taken together, these results argue an FLT3-ITD-targeted mechanism of anti-proliferative action within leukaemic cells, which is consistent with previous observations [35,37].

Table 3
Inhibitory effect of **12b** and **12r** on a panel of FLT3-mutated isoforms.

FLT3 mutant	Kinase inhibition, K_i (μM)[a]	
	12b	12r
FLT3 (ITD)	0.002	0.0002
FLT3 (ITD)-NPOS	0.262	<0.0003
FLT3 (ITD)-W51	0.084	<0.0003
FLT3 (D835Y)	0.047	<0.0003
FLT3 (Y591-V592insVDFREYEYD)	0.185	<0.0003
FLT3 (F594_R595insR)	0.054	<0.0003
FLT3 (F594_R595insREY)	0.064	<0.0003
FLT3 (R595_E596insEY)	0.077	<0.0003

[a] Apparent inhibition constants (K_i) were determined by Reaction Biology Corporation; K_i values were calculated using the half maximal inhibition (IC_{50}) and the appropriate K_m(ATP) of each FLT3 mutant.

2.6. Cellular mechanistic studies

To decipher the plausible cellular mechanism of their anti-proliferative action, compounds **12b** and **12r** were assessed against MV4-11, a sensitive cell line with *FLT3*-ITD mutation, and U937, a non-sensitive cell line with low expression of WT FLT3 only, using annexin V/propidium iodide (PI) assays and western blotting analysis.

Firstly, annexin V/PI double staining was carried out to examine the apoptotic effects of each compound at concentrations of 1 ×, 5 ×, 10 × and 20 × its 24 h GI_{50} value (that was determined in MV4-11 cells using the 24 h resazurin assay, *i.e.*, **12b**: 24 h GI_{50} = 0.125 μM and **12r**: 24 h GI_{50} = 0.085 μM) after incubation with either cell line (MV4-11 or U937) for a period of 24 or 48 h. Compound **12b** was capable of inducing apoptosis of MV4-11 cells in a concentration-dependent manner, with the effect being more profound at later time point (Fig. 5). For example, in comparison with DMSO diluent, **12 b** at the highest concentration (*i.e.*, 20 × GI_{50}) triggered approximately 9% and 26% more apoptotic cells after 24- and 48-h treatments, respectively (Fig. 5A and B); this effect was almost wholly attributed to the late apoptosis (Fig. 5C). Compound **12r** exerted the apoptosis-inducing effect on MV4-11 cells to a similar extent as **12b** (Fig. S1). In contrast, neither compound caused apparent apoptosis of U937 cells at all four concentrations. Collectively, these data are in agreement with GI_{50} values of compounds **12r** and **12b** obtained from 72 h cell viability assays using resazurin (Table 4), supporting that apoptosis contributes to the anti-proliferative effects of the two compounds on MV4-11 cells.

To understand the mechanism underlying the induction of apoptosis described above as well as to investigate the cellular FLT3 inhibitory potency of **12b** and **12r**, MV4-11 and U937 cells were

Table 4
Anti-proliferative activities of **12b** and **12r** against multiple leukaemic cell lines.

Human leukaemia cell line	FLT3 status	Growth inhibition, GI_{50} (μM)[a]	
		12b	12r
MV4-11	FLT3-ITD	0.074 ± 0.010	0.017 ± 0.012
MOLM-13	FLT3-ITD	0.023 ± 0.001	0.0004 ± 0.0002
NB4	FLT3-WT	1.060 ± 0.080	0.126 ± 0.041
THP1	FLT3-WT	7.720 ± 3.949	3.037 ± 3.351
U937	FLT3-WT/low	>10	>10
Jurkat	FLT3-null	>10	>10
K562	FLT3-null	>10	0.185 ± 0.055

[a] GI_{50} values were determined using 72 h resazurin assays and are presented as mean ± SD derived from at least two replicates.

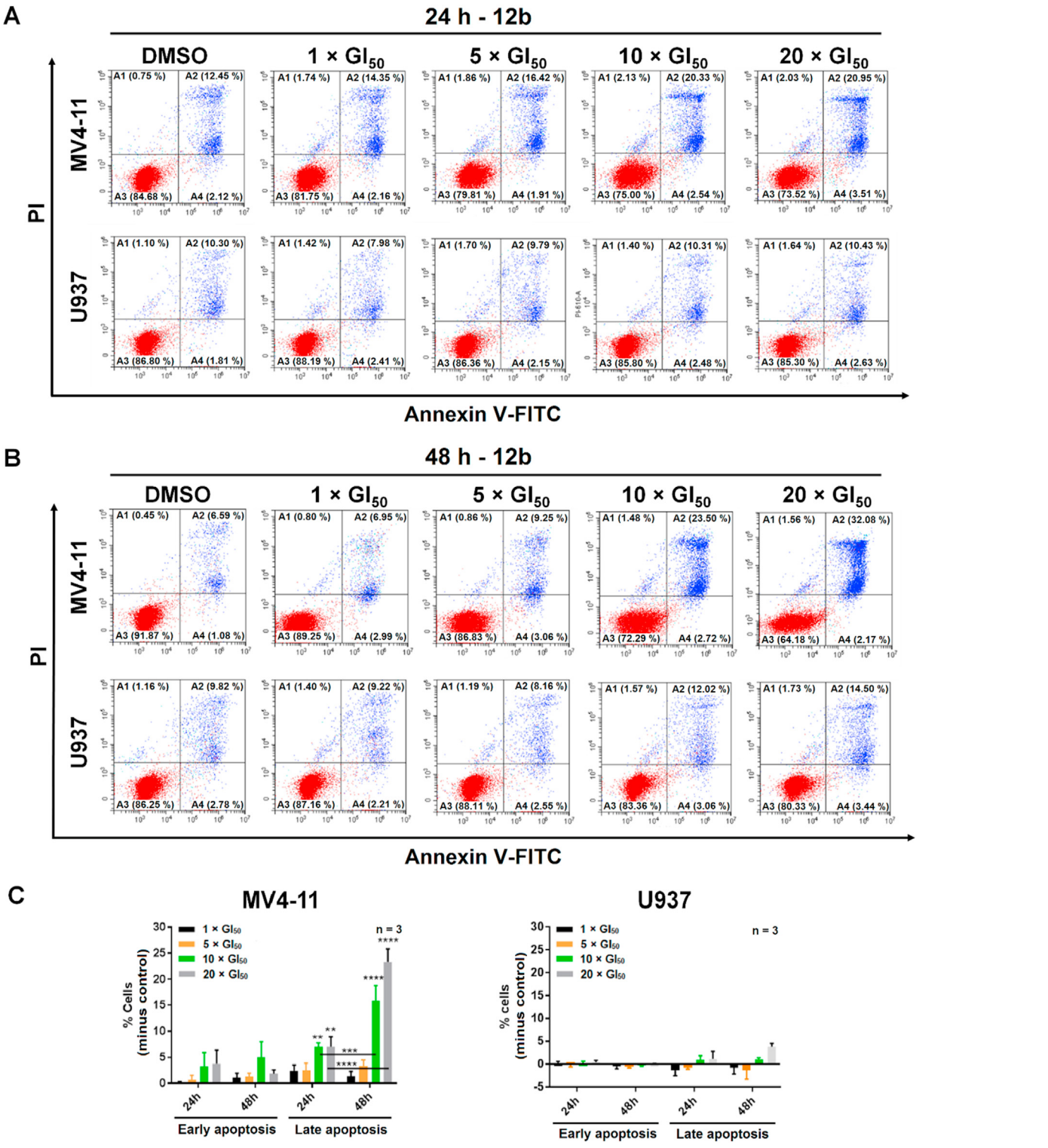

Fig. 5. Detection of apoptosis of MV4-11 or U937 cells after incubation with **12b** for 24 (**A**) or 48 (**B**) hours using annexin V/PI double staining assays, followed by quantitative analysis (**C**). GI_{50} in the figure refers to the 24 h value of MV4-11 cells (*i.e.*, 0.125 μM). Independent experiments were conducted in triplicate. Statistical analysis was performed using GraphPad one-way ANOVA analysis with Tukey's post-hoc test, and statistical significance defined as a *p*-value of <0.05 (*), <0.01 (**), <0.001 (***) or < 0.0001 (****) (GraphPad Prism v.7, La Jolla, CA, USA).

individually incubated with each compound at concentrations of 1 ×, 10 × and 20 × GI_{50}(24 h, MV4-11) for 6 or 24 h, and analysed using western blotting (Fig. 6 and Fig. S2). As mentioned previously, autophosphorylated FLT3 lies upstream of three oncogenic pathways, namely JAK/STAT5, RAS/RAF/MEK/ERK and PI3K/AKT/mTOR [13,15]. To determine the effect of **12b** on these signalling pathways, several key pathway components were examined for their total and phosphorylated levels. As shown in Figs. 6, **12b** was capable of significantly reducing, if not abolishing, FLT3-driven phosphorylation of STAT5, ERK, AKT, S6RP and eIF4E (the last two are

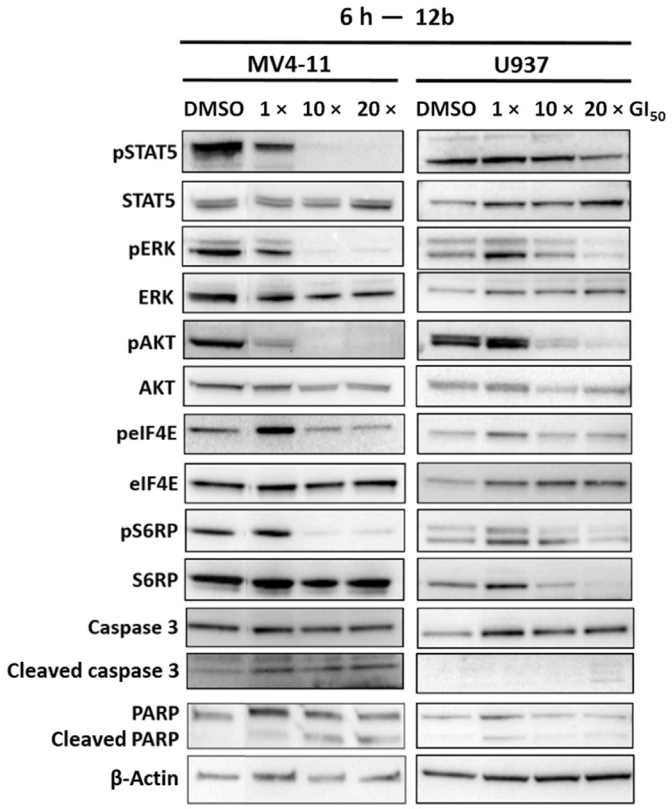

Fig. 6. Western blot analysis of MV4-11 and U937 cells treated with **12b** for a period of 6 h. GI_{50} in the figure refers to the 24 h value of MV4-11 cells (*i.e.*, 0.125 μM). DMSO diluent was used as control in each experiment, and β-actin as a loading control. The blots present the results of at least two independent experiments.

downstream effectors of mTOR) [40–43] at no expense of their respective total levels after 6-h incubation with MV4-11 cells, indicating that FLT3-mediated signalling pathways were greatly dampened or even blocked by this compound. These suppressive effects were also found in U937 cells treated with **12b**, but in a much weaker manner at each of the same compound concentrations as used in MV4-11 cells. In addition, **12b** increased the cleavages of poly(ADP-ribose)polymerase (PARP) and caspase-3 in MV4-11 cells, but these cleavages were nearly not detectable in U937 cells. However, the level of anti-apoptotic protein myeloid cell leukaemia 1 (Mcl-1) was downregulated in both cell lines after 24-h incubation with either **12b** or **12r**, with the reducing effect being far more marked in MV4-11 cells than that in U937 cells (Fig. S2). These results correlate well with the observations obtained from cell viability and apoptosis assays, suggesting the anti-proliferative effects of **12b** and **12r** on MV4-11 cells could originate from their inhibition of FLT3-ITD.

3. Conclusions

Capitalising on the serendipitous discovery of **12b** as an FLT3 inhibitor, the utility and versatility of its core scaffold, *i.e.*, *N*-phenylpyrimidin-2-amine, for the fabrication of novel, potent and selective FLT3 inhibitors were explored using an analogue-based design approach. A series of 4-azaaryl-*N*-phenylpyrimidin-2-amine derivatives was synthesised, and their structure-activity relationships were analysed. All of these compounds displayed nanomolar potencies against FLT3-ITD with one third of them being sub-nanomolar inhibitors; these potencies were well reflected in their anti-proliferative effects on *FLT3*-ITD-harbouring MV4-11 cells. Further profiling of **12b** and **12r** using a panel of seven additional FLT3 mutants and a selection of six extra leukaemic cell lines with different FLT3 statuses revealed their board FLT3 inhibitory spectra and high anti-proliferative specificity for the cell lines with ITD mutation, respectively. The hit compound **12b** with a decent selectivity for FLT3-ITD was capable of inducing apoptosis and downregulating the phosphorylation of key downstream effectors of FLT3 in MV4-11 cells, substantiating the FLT3-ITD-targeted mechanism of its anti-proliferative action.

4. Experimental

4.1. Docking studies

The potential modes of the binding of **12b** to FLT3 were investigated with Schrödinger suite docking program, Glide, under the Maestro graphical user interface. Other associated programs included LigPrep and Protein Preparation Wizard. *Preparing 3D conformers using LigPrep*: the 3D conformers of **12b** were generated by LigPrep with default settings. *Docking using Glide*: the first step of performing structure-based docking was to generate the receptor grid for FLT3. The required atomic coordinates of FLT3 were obtained from the Protein Data Bank (PDB ID: 4RT7) and loaded onto the Maestro interface. Any missing atoms in the structures were added using Protein Preparation Wizard. Whilst retaining the default settings, the docking receptor was defined and generated with the centre at the ATP-binding pocket. Subsequently, the prepared conformers of **12b** were docked into the ATP-binding site of FLT3 using Glide. During the docking process, the extra precision mode was selected, and the number of energy minimisation steps was maximised to 400 to ensure convergence. The results were ranked according to the Glide-XP docking score, and the best scoring pose was analysed in Maestro and viewed with PyMOL.

4.2. Chemistry

Chemical reagents and solvents including anhydrous solvents were purchased from commercial sources, and used as received unless specified otherwise. All reactions except microwave-assisted syntheses were carried out with continuous magnetic stirring in ordinary glassware; microwave-assisted syntheses were performed in a 10 mL Asynt DrySyn insert (Isleham, UK) using a CEM Discover SP and Explorer 48/72/96 microwave system (Matthews, NC, USA) controlled by Synergy™ software (Firmware version DSCA02.17). Heating of reactions was conducted with a DrySyn® single- or multi-position heating block (Isleham, UK); cooling of reactions was achieved using an ice bath. Analytical TLC was performed on Merck silica gel 60 F_{254} pre-coated aluminium plates (0.2 mm) and visualised under UV light (254 nm). Flash column chromatography was carried out using a fritted solid loader packed with GRACE Davison DAVISIL® silica gel 60 Å (40–63 μm) on a Biotage Flash-Master Personal^{+} flash chromatography system or using a conventional glass column. ^{1}H and ^{13}C NMR spectra were recorded at 298 K (unless otherwise specified) on a Bruker AVANCE III HD 500 spectrometer (^{1}H at 500.20 MHz and ^{13}C at 125.79 MHz; Faellanden, Switzerland), and were analysed using Bruker Topspin 3.2 software. ^{1}H and ^{13}C NMR spectra are referenced to ^{1}H signals of residual nondeuterated solvents and ^{13}C signals of deuterated solvents, respectively. ^{1}H NMR signals are reported with chemical shift values δ (ppm), multiplicity (s = singlet, d = doublet, t = triplet, dd = doublet of doublets, td = triplet of doublets, ddd = doublet of doublet of doublets, m = multiplet and br = broad), relative integral, coupling constants J (Hz) and assignments. High resolution mass spectra were recorded on an AB SCIEX TripleTOF 5600 mass spectrometer (Concord, ON, Canada), and ionisation of all samples

was carried out using ESI. Melting points were determined using an open capillary on a Stuart SMP10 or Mettler Toledo MP50 melting point apparatus, and are uncorrected. The purity of compounds used for biological evaluation was determined by analytic RP-HPLC which was carried out on a Shimadzu Prominence UltraFast Liquid Chromatograph (UFLC) system (Kyoto, Japan) equipped with a CBM-20A communications bus module, a DGU-20A5R degassing unit, an LC-20AD liquid chromatograph pump, an SIL-20AHT autosampler, an SPD-M20A photo diode array detector, a CTO-20A column oven and a Phenomenex Kinetex 5u C18 100A 250 mm × 4.60 mm column. Method A (gradient 5%–95% CH_3OH containing 0.1% formic acid (FA) over 20 min at a flow rate of 1 mL/min, followed by 95% CH_3OH containing 0.1% FA over 5 min), and method B (gradient 5%–95% CH_3CN containing 0.1% FA over 20 min at a flow rate of 1 mL/min, followed by 95% CH_3CN containing 0.1% FA over 5 min) were used for analytic RP-HPLC. Data acquired from analytic RP-HPLC were processed using LabSolutions Analysis Data System.

General synthetic procedure A: acetylation of (aza)indoles.

(i) To a solution of an indole (1.00 equiv.) in acetic anhydride (1 M in indole) was added cyanoacetic acid (1.18 equiv.), and the reaction mixture was heated at 85 °C for 10 min, cooled down to room temperature. The crystals thus formed were filtered, washed with CH_3OH (50 mL) and dried under reduced pressure to give the desired 3-acetylindole.

(ii) To a suspension of $AlCl_3$ (5.0 equiv.) in anhydrous DCM (100 mM in azaindole) under N_2 was added an azaindole (1.0 equiv.). The reaction mixture was stirred at room temperature for 1 h, and acetyl chloride (5.0 equiv.) was added dropwise. The reaction mixture was stirred at room temperature overnight, cooled down on an ice bath for 15 min, quenched by slow addition of CH_3OH (150 mL), stirred at room temperature for 1 h, and concentrated under reduced pressure. The residue was dissolved in H_2O (50 mL), basified to pH 12 with 2 M NaOH, and extracted with EtOAc (3 × 200 mL) and DCM (3 × 200 mL). The organic extracts were combined and concentrated under reduced pressure, and the residue was purified by flash column chromatography (silica gel, DCM ramping to DCM:CH_3OH = 92:8) to give the desired 3-acetylazaindole.

General synthetic procedure B: formation of enaminones.

(i) To DMF-DMA (1.20 equiv.) was added a ketone (1.00 equiv.). The reaction mixture was stirred at room temperature for 5 min, filtered and crystallised with EtOH to afford the desired enaminone.

(ii) To DMF-DMA (5.00–10.0 equiv.) was added a ketone (1.00 equiv.). The reaction mixture was heated at reflux for 2–36 h, concentrated under reduced pressure, and either crystallised with EtOH or washed with Et_2O to afford the desired enaminone.

(iii) To DMF-DMA (3.00–5.00 equiv.) was added a ketone (1.00 equiv.). The reaction mixture was heated under microwave at 180 °C for 1 h, concentrated under reduced pressure, and purified by flash column chromatography (silica gel, DCM ramping to DCM/CH_3OH = 9:1) to give the desired enaminone.

(iv) To 1-*tert*-butoxy-*N*,*N*,*N*′,*N*′-tetramethylmethanediamine (2.00 equiv.) was added a ketone (1.00 equiv.). The reaction mixture was heated at reflux for 6 h, and concentrated *via* forced evaporation under a stream of air and *in vacuo*. The residue was washed with DCM (3 × 6 mL) to give the desired enaminone.

General synthetic procedure C: reduction of nitro compounds to amines

To a suspension of a nitro compound (1.0 equiv.) in CH_3OH (50 mM in the nitro compound) was added 10% Pd/C (0.01 equiv.). The reaction mixture was bubbled with H_2 gas at room temperature for 30 min, stirred under H_2 overnight, and filtered through a pad of Celite®. The solids were washed with CH_3OH (300 mL). The filtrate and washing were combined and concentrated under reduced pressure to give the desired amine.

General synthetic procedure D: guanidinylation of amines

To a solution of an amine (1.0 equiv.) and cyanamide (2.0 equiv.) in CH_3CN (100 mL) on an ice bath was added TMSCl (2.0 equiv.) dropwise. The reaction mixture was heated at reflux overnight and filtered while hot. The precipitate was washed with Et_2O or EtOAc (100–150 mL) to give the desired guanidine.

General synthetic procedure E: formation of pyrimidines

To a solution of a guanidine (2.0 equiv.) in CH_3CN or 2-methoxyethanol (4 mL) were added an enaminone (1.0 equiv.) and NaOH (2.0 equiv.). The reaction mixture was heated at 160 °C under microwave irradiation for 1 h, cooled down to room temperature and concentrated under reduced pressure. The residue was purified by FlashMaster Personal$^+$ chromatography or glass column (silica gel) and washed with ice-cold CH_3OH or EtOAc (3 × 5 mL) to give the desired pyrimidine.

3-(1*H*-indol-3-yl)-3-oxopropanenitrile (2a)

Indole (**1a**, 5.86 g, 50.0 mmol) and cyanoacetic acid (5.00 g, 58.8 mmol) were reacted according to general synthetic procedure A(i) to give **2a** as an off-white solid (8.29 g, 90%). **^{1}H NMR** (DMSO-d_6) δ 4.49 (s, 2H, CH_2), 7.22–7.27 (m, 2H, indolyl-H), 7.50–7.51 (d, 1H, *J* 7.0, indolyl-H), 8.14 (d, 1H, *J* 7.0, indolyl-H), 8.37 (s, 1H, indolyl-H), 12.18 (br s, 1H, indolyl-NH). **HRMS** (ESI-TOF) *m/z* 185.0713 $[M+H]^+$; calcd. for $C_{11}H_9N_2O^+$ 185.0709 $[M+H]^+$.

3-(2-Methyl-1*H*-indol-3-yl)-3-oxopropanenitrile (2b)

2-Methylindole (**1b**, 6.56 g, 50.0 mmol) and cyanoacetic acid (5.00 g, 58.8 mmol) were reacted according to general synthetic procedure A(i) to give **2B** as an off-white solid (9.12 g, 92%). **^{1}H NMR** (DMSO-d_6) δ 2.68 (s, 3H, CH_3), 4.52 (s, 2H, CH_2), 7.15–7.19 (m, 2H, indolyl-H), 7.39 (d, 1H, *J* 7.0, indolyl-H), 7.97 (d, 1H, *J* 7.0, indolyl-H), 12.09 (br s, 1H, indolyl-NH). **HRMS** (ESI-TOF) *m/z* 199.0867 $[M+H]^+$; calcd. for $C_{12}H_{11}N_2O^+$ 199.0866 $[M+H]^+$.

1-(1-Tosyl-1*H*-indol-3-yl)ethan-1-one (2d)

To a solution of 3-acetylindole (**2c**, 15.9 g, 100 mmol) and tetrabutylammonium hydrogen sulfate (3.40 g, 10.0 mmol) in DCM was added 50% (w/v) NaOH (60 mL, 750 mmol) slowly and stirred vigorously at room temperature for 15 min. 4-Toluenesulfonyl chloride (28.9 g, 150 mmol) was added slowly in portions and stirred vigorously at room temperature overnight. The reaction mixture was poured into H_2O (100 mL), and extracted with DCM (3 × 100 mL). The organic extracts were combined, dried over Na_2SO_4 and concentrated under reduced pressure. The resulting oil was crystallised upon standing to yield **2d** as an off-white solid (31.1 g, 99%) which was used in the next step without further purification. **^{1}H NMR** (DMSO-d_6) δ 2.31 (s, 3H, tosyl-CH_3), 2.60 (s, 3H, acetyl-CH_3), 7.35 (td, 1H, *J* 8.0 & 1.0, indolyl-H), 7.38 (td, 1H, *J* 8.0 & 1.0, indolyl-H), 7.41 (d, 2H, *J* 8.0, tosyl-H), 7.94 (d, 1H, *J* 8.0, indolyl-H), 8.03 (d, 2H, *J* 8.0, tosyl-H), 8.19 (d, 1H, *J* 8.0, indolyl-H), 8.79 (s, 1H, indolyl-H). **HRMS** (ESI-TOF) *m/z* 314.0849 $[M+H]^+$; calcd. for $C_{17}H_{16}NO_3S^+$ 314.0845 $[M+H]^+$.

1-(1*H*-Pyrrolo[3,2-*b*]pyridin-3-yl)ethan-1-one (4a)

4-Azaindole (**3a**, 2.36 g, 20.0 mmol) and acetyl chloride (7.10 mL, 99.9 mmol) were reacted according to general synthetic procedure A(ii) to give **4a** as a white solid (2.64 g, 82%). **^{1}H NMR** (DMSO-d_6) δ 2.72 (s, 3H, CH_3), 7.23 (dd, 1H, *J* 8.0 & 4.5, azaindolyl-H), 7.88 (dd, 1H, *J* 8.0 & 1.5, azaindolyl-H), 8.29 (s, 1H, azaindolyl-H), 8.50 (dd, 1H,

J 4.5 & 1.5, azaindolyl-H) (one proton signal (azaindolyl-NH) not observed). **HRMS** (ESI-TOF) *m/z* 161.0709 $[M+H]^+$; calcd. for $C_9H_9N_2O^+$ 161.0709 $[M+H]^+$.

1-(1*H*-Pyrrolo[2,3-*b*]pyridin-3-yl)ethan-1-one (4b)

7-Azaindole (**3b**, 5.91 g, 50.0 mmol) and acetyl chloride (17.8 mL, 250 mmol) were reacted according to general synthetic procedure A(ii) to give **4b** as a beige solid (6.15 g, 77%). **^{1}H NMR** (DMSO-d_6) δ 2.46 (s, 3H, CH_3), 7.23 (dd, 1H, *J* 7.5 & 5.0, azaindolyl-H), 8.31 (dd, 1H, *J* 5.0 & 1.5, azaindolyl-H), 8.45 (s, 1H, azaindolyl-H), 8.46 (dd, 1H, *J* 7.5 & 1.5, azaindolyl-H), 12.42 (br s, 1H, azaindolyl-NH). **HRMS** (ESI-TOF) *m/z* 161.0700 $[M+H]^+$; calcd. for $C_9H_9N_2O^+$ 161.0709 $[M+H]^+$.

1-(1-Methyl-1*H*-pyrrolo[2,3-*b*]pyridin-3-yl)ethan-1-one (4c) & 1-(7-methyl-7*H*-pyrrolo[2,3-*b*]pyridin-3-yl)ethan-1-one (4d)

To DMF-DMA (4.00 mL, 30.1 mmol) was added **4b** (1.61 g, 10.0 mmol). The reaction mixture was heated at reflux overnight and concentrated under reduced pressure. The residue was purified by FlashMaster Personal$^+$ chromatography (silica gel, DCM ramping to DCM:CH_3OH = 95:5) to give **4c** as a beige solid (891 mg, 51%) and **4d** as a beige solid (457 mg, 26%).

4c: **^{1}H NMR** (DMSO-d_6) δ 2.44 (s, 3H, $COCH_3$), 3.87 (s, 3H, azaindolyl-NCH_3), 7.28 (dd, 1H, *J* 7.5 & 4.5, azaindolyl-H), 8.37 (dd, 1H, *J* 4.5 & 1.5, azaindolyl-H), 8.46 (dd, 1H, *J* 7.5 & 1.5, azaindolyl-H), 8.52 (s, 1H, azaindolyl-H). **HRMS** (ESI-TOF) *m/z* 175.0878 $[M+H]^+$; calcd. for $C_{10}H_{11}N_2O^+$ 175.0866 $[M+H]^+$.

4d: **^{1}H NMR** (DMSO-d_6) δ 2.43 (s, 3H, $COCH_3$), 4.29 (s, 3H, azaindolyl-NCH_3), 7.26 (dd, 1H, *J* 7.5 & 6.5, azaindolyl-H), 8.28 (d, 1H, *J* 6.0, azaindolyl-H), 8.44 (s, 1H, azaindolyl-H), 8.69 (dd, 1H, *J* 7.5 & 1.0, azaindolyl-H). **HRMS** (ESI-TOF) *m/z* 175.0841 $[M+H]^+$; calcd. for $C_{10}H_{11}N_2O^+$ 175.0866 $[M+H]^+$.

N-Methoxy-*N*-methyl-1*H*-indazole-3-carboxamide (6a)

To a solution of 1*H*-indazole-3-carboxylic acid (**5**, 4.87 g, 30.0 mmol) in THF (250 mL) was added *N*,*O*-dimethylhydroxylamine hydrochloride (3.22 g, 33.0 mmol) at room temperature. The reaction mixture was cooled on an ice-salt bath for 30 min, and pyridine (5.34 mL, 66.0 mmol) was added. The resultant reaction mixture was stirred on the ice-salt bath for 2 h and at room temperature for 1 h. Pyridine (5.34 mL, 66.0 mmol) and EDC·HCl (11.5 g, 60.0 mmol) were added. The reaction mixture was stirred at room temperature overnight and concentrated under reduced pressure, and the residue was triturated with H_2O (500 mL). The solids were filtered and washed with H_2O (400 mL) to give **6a** as a white solid (5.26 g, 85%). **^{1}H NMR** ($CDCl_3$) δ 3.57 (s, 3H, NCH_3), 3.81 (s, 3H, OCH_3), 7.24–7.28 (m, 1H, indazolyl-H), 7.39–7.43 (m, 1H, indazolyl-H), 7.55 (d, 1H, *J* 8.5, indazolyl-H), 8.21 (d, 1H, *J* 8.0, indazolyl-H), 11.24 (br s, 1H, indazolyl-NH). **HRMS** (ESI-TOF) *m/z* 206.0927 $[M+H]^+$; calcd. for $C_{10}H_{12}N_3O_2^+$ 206.0924 $[M+H]^+$.

Tert-butyl 3-(methoxy(methyl)carbamoyl)-1*H*-indazole-1-carboxylate (6b)

To a solution of **6a** (4.10 g, 20.0 mmol) in DCM (250 mL) on an ice-salt bath were added DMAP (489 mg, 4.00 mmol), triethylamine (5.58 mL, 40.0 mmol) and di-*tert*-butyl dicarbonate (8.73 g, 40.0 mmol). The reaction mixture was stirred on the ice-salt bath for 1 h and at room temperature overnight, washed with 0.5 M HCl (100 mL), H_2O (100 mL) and brine (100 mL), dried over Na_2SO_4, and concentrated under the reduced pressure. The residue was purified by flash column chromatography (silica gel, petroleum benzine ramping to petroleum benzine:EtOAc = 7:3) to give **6b** as a white solid (5.98 g, 98%). **^{1}H NMR** ($CDCl_3$) δ 1.67 (s, 9H, $C(CH_3)_3$), 3.43 (br s, 3H, NCH_3), 3.86 (s, 3H, OCH_3), 7.32 (app t, 1H, *J* 8.0, indazolyl-H), 7.49 (ddd, 1H, *J* 8.0 & 7.0 &1.0, indazolyl-H), 8.08 (app br s, 1H, indazolyl-H), 8.11 (d, 1H, *J* 8.5, indazolyl-H). **HRMS** (ESI-TOF) *m/z* 633.2660 $[2M+Na]^+$; calcd. for $C_{30}H_{38}N_6NaO_8^+$ 633.2643 $[2M+Na]^+$.

1-(1*H*-indazol-3-yl)ethan-1-one (7a)

A solution of **6a** (8.21 g, 40.0 mmol) in anhydrous THF (150 mL) under N_2 was cooled down on an acetone-dry ice bath for 30 min, and methyl magnesium bromide (3.0 M in diethyl ether, 33.4 mL, 100 mmol) was added. The reaction mixture was stirred on the acetone-dry ice bath for 2.5 h and at room temperature for 1 h, quenched with saturated aqueous NH_4Cl solution (50 mL), extracted with EtOAc (2 × 100 mL). The organic extracts were combined and concentrated under reduced pressure, and the residue was purified by flash column chromatography (silica gel, DCM ramping to DCM:MeOH = 98:2) to give **7a** as a white solid (6.09 g, 95%). **^{1}H NMR** ($CDCl_3$) δ 2.76 (s, 3H, CH_3), 7.35 (ddd, 1H, *J* 8.0 & 7.0 & 1.0, indazolyl-H), 7.46 (ddd, 1H, *J* 8.0 & 7.0 & 1.0, indazolyl-H), 7.55 (d, 1H, *J* 8.5, indazolyl-H), 8.40 (dt, 1H, *J* 8.0 & 1.0, indazolyl-H), 10.49 (br s, 1H, indazolyl-NH). **HRMS** (ESI-TOF) *m/z* 161.0709 $[M+H]^+$; calcd. for $C_9H_9N_2O^+$ 161.0709 $[M+H]^+$.

3-(1*H*-indazol-3-yl)-3-oxopropanenitrile (7b)

To a solution of **6b** (2.75 g, 9.01 mmol) in anhydrous THF (50 mL) under N_2 was added anhydrous CH_3CN (706 μL, 13.5 mmol). The reaction mixture was cooled down on an acetone-dry ice bath for 30 min, and lithium diisopropylamide (2.0 M in THF/heptane/ethylbenzene, 6.75 mL, 13.5 mmol) was added dropwise over 15 min. The reaction mixture was stirred on the acetone-dry ice bath for 2 h and at room temperature overnight, quenched with H_2O (10 mL), acidified with 2.0 M HCl to pH 1, extracted with $CHCl_3$ (3 × 100 mL). The organic extracts were combined and concentrated under the reduced pressure, the residue was purified by FlashMaster Personal$^+$ chromatography (silica gel, DCM ramping to DCM:EtOAc = 9:1) to give **7b** as a beige solid (1.36 g, 81%). **^{1}H NMR** ($CDCl_3$) δ 4.31 (s, 2H, CH_2), 7.41 (ddd, 1H, *J* 8.0 & 7.0 & 1.0, indazolyl-H), 7.52 (ddd, 1H, *J* 8.0 & 7.0 &1.0, indazolyl-H), 7.59 (d, 1H, *J* 8.5, indazolyl-H), 8.34 (d, 1H, *J* 8.5, indazolyl-H), 10.50 (br s, 1H, indazolyl-NH). **HRMS** (ESI-TOF) *m/z* 186.0667 $[M+H]^+$; calcd. for $C_{10}H_8N_3O^+$ 186.0662 $[M+H]^+$.

3-(Dimethylamino)-2-(1*H*-indole-3-carbonyl)acrylonitrile (8a)

2a (1.85 g, 10.0 mmol) and DMF-DMA (1.50 mL, 11.3 mmol) were reacted according to general synthetic procedure B(i) to afford **8a** as a yellow solid (2.31 g, 96%). **^{1}H NMR** (DMSO-d_6) δ 3.27 (s, 3H, NCH_3), 3.37 (s, 3H, NCH_3), 7.12–7.20 (m, 2H, indolyl-H), 7.47 (d, 1H, *J* 8.0, indolyl-H), 8.00 (s, 1H, NCH=C(CO)CN), 8.13 (d, 1H, *J* 8.0, indolyl-H), 8.27 (s, 1H, indolyl-H), 11.76 (br s, 1H, indolyl-NH). **HRMS** (ESI-TOF) 240.1130 ($[M+H]^+$); calcd. for $C_{14}H_{14}N_3O^+$ ($[M+H]^+$) 240.1131.

3-(Dimethylamino)-2-(1-methyl-1*H*-indole-3-carbonyl)acrylonitrile (8b)

2a (478 mg, 3.00 mmol) and DMF-DMA (4.30 mL, 32.4 mmol) were reacted according to general synthetic procedure B(ii) in the presence of DMF (6 mL). The residue was crystallised with EtOH (5 mL) to afford **8b** as a yellow solid (545 mg, 81%). **^{1}H NMR** (DMSO-d_6) δ 3.27 (s, 3H, CH_3NCH_3), 3.36 (s, 3H, CH_3NCH_3), 3.86 (s, 3H, indolyl-NCH_3), 7.18–7.28 (m, 2H, indolyl-H), 7.52 (d, 1H, *J* 8.0, indolyl-H), 7.99 (s, 1H, NCH=C(CO)CN), 8.14 (d, 1H, *J* 7.5, indolyl-H), 8.24 (s, 1H, indolyl-H). **HRMS** (ESI-TOF) 254.1311 ($[M+H]^+$); calcd. for $C_{15}H_{16}N_3O^+$ ($[M+H]^+$) 254.1288.

3-(Dimethylamino)-2-(2-methyl-1*H*-indole-3-carbonyl)acrylonitrile (8c)

2b (1.98 g, 10.0 mmol) and DMF-DMA (1.50 mL, 11.3 mmol) were reacted according to general synthetic procedure B(i) to afford **8c** as a yellow solid (2.48 g, 98%). **^{1}H NMR** (DMSO-d_6) δ 2.50 (s, 3H, indolyl-CH_3), 3.20 (s, 3H, NCH_3), 3.35 (s, 3H, NCH_3), 7.02–7.09 (m, 2H, indolyl-H), 7.31 (d, 1H, *J* 8.0, indolyl-H), 7.56 (d, 1H, *J* 8.0, indolyl-H), 7.74 (s, 1H, NCH=C(CO)CN), 11.56 (br s, 1H, indolyl-NH). **HRMS** (ESI-TOF) 254.1269 ($[M+H]^+$); calcd. for $C_{15}H_{16}N_3O^+$ ($[M+H]^+$) 254.1288.

3-(Dimethylamino)-1-(1-methyl-1*H*-indol-3-yl)prop-2-en-1-one (8d)

3-Acetylindole (**2c**, 5.00 g, 31.4 mmol) and DMF-DMA (45.0 mL,

339 mmol) were reacted according to general synthetic procedure B(ii) in the presence of DMF (63 mL). The residue was crystallised with EtOH (20 mL) to afford **8d** as a yellow solid (5.45 g, 76%). **^{1}H NMR** (DMSO-d_6) δ 2.96 (s, 6H, CH_3NCH_3), 3.82 (s, 3H, indolyl-NCH_3), 5.72 (d, 1H, *J* 12.5, CH=C*H*CO), 7.14 (t, 1H, *J* 7.5, indolyl-H), 7.20 (t, 1H, *J* 7.5, indolyl-H), 7.46 (d, 1H, *J* 8.0, indolyl-H),7.54 (d, 1H, *J* 12.5, C*H*=CHCO), 8.16 (s, 1H, indolyl-H), 8.30 (d, 1H, *J* 8.0, indolyl-H). **HRMS** (ESI-TOF) 229.1339 ([M+H]$^+$); calcd. for $C_{14}H_{17}N_2O^+$ ([M+H]$^+$) 229.1335.

3-(Dimethylamino)-1-(1-tosyl-1*H*-indol-3-yl)prop-2-en-1-one (8e)

2d (3.13 g, 10.0 mmol) and DMF-DMA (3.0 mL, 22.6 mmol) were reacted according to general synthetic procedure B(ii). The solid thus formed was filtered and washed with Et_2O to afford **8e** as a yellow solid (2.87 g, 78%). **^{1}H NMR** (DMSO-d_6) δ 2.32 (s, 3H, tosyl-CH_3), 3.10 (s, 6H, CH_3NCH_3), 5.93 (d, 1H, *J* 12.5, CH=C*H*CO), 7.11 (d, 2H, *J* 8.0, tosyl-H), 7.29 (td, 1H, *J* 8.0 & 1.0, indolyl-H), 7.35 (td, 1H, *J* 8.0 & 1.0, indolyl-H), 7.48 (d, 1H, *J* 8.0, indolyl-H), 7.64 (d, 1H, *J* 12.5, C*H*=CHCO), 7.95 (d, 2H, *J* 8.0, tosyl-H), 8.30 (d, 1H, *J* 8.0, indolyl-H), 8.61 (s, 1H, indolyl-H). **HRMS** (ESI-TOF) 369.1274 ([M+H]$^+$); calcd. for $C_{20}H_{21}N_2O_3S^+$ ([M+H]$^+$) 369.1267.

(*E*)-3-(Dimethylamino)-1-(1*H*-pyrrolo[2,3-*b*]pyridin-3-yl)prop-2-en-1-one (8f)

4a (2.56 g, 16.0 mmol) and 1-*tert*-butoxy-*N*,*N*,*N*′,*N*′-tetramethylmethanediamine (6.53 mL, 32.0 mmol) were reacted according to general synthetic procedure B(iv) to give **8f** as a dark brown solid (2.38 g, 69%). **^{1}H NMR** (DMSO-d_6) δ 2.96 (br s, 3H, CH_3), 3.07 (br s, 3H, CH_3), 6.83 (d, 1H, *J* 12.5, CH=C*H*CO), 7.16 (dd, 1H, *J* 8.5 & 4.5, azaindolyl-H), 7.69 (d, 1H, *J* 12.5, C*H*=CHCO), 7.83 (dd, 1H, *J* 8.5 & 1.5, azaindolyl-H), 8.12 (s, 1H, azaindolyl-H), 8.46 (dd, 1H, *J* 4.5 & 1.5, azaindolyl-H) (one proton signal (azaindolyl-NH) not observed). **HRMS** (ESI-TOF) *m/z* 216.1134 [M+H]$^+$; calcd. for $C_{12}H_{14}N_3O^+$ 216.1131 [M+H]$^+$.

(*E*)-3-(Dimethylamino)-1-(1*H*-pyrrolo[2,3-*b*]pyridin-3-yl)prop-2-en-1-one (8g)

4b (1.61 g, 10.0 mmol) and 1-*tert*-butoxy-*N*,*N*,*N*′,*N*′-tetramethylmethanediamine (4.13 mL, 20.0 mmol) were reacted according to general synthetic procedure B(iv) to give **8g** as a beige solid (1.83 g, 85%). **^{1}H NMR** (DMSO-d_6) δ 2.98 (br s, 6H, CH_3NCH_3), 5.80 (d, 1H, *J* 12.5, CH=C*H*CO), 7.15 (dd, 1H, *J* 7.5 & 4.5, azaindolyl-H), 7.56 (d, 1H, *J* 12.5, C*H*=CHCO), 8.24 (dd, 1H, *J* 4.5 & 1.5, azaindolyl-H), 8.29 (s, 1H, azaindolyl-H), 8.54 (dd, 1H, *J* 7.5 & 1.5, azaindolyl-H), 12.11 (br s, 1H, azaindolyl-NH). **HRMS** (ESI-TOF) *m/z* 216.1137 [M+H]$^+$; calcd. for $C_{12}H_{14}N_3O^+$ 216.1131 [M+H]$^+$.

(*E*)-3-(Dimethylamino)-1-(1-methyl-1*H*-pyrrolo[2,3-*b*]pyridin-3-yl)prop-2-en-1-one (8h)

4c (732 mg, 4.20 mmol) and DMF-DMA (3.00 mL, 22.6 mmol) were reacted according to general synthetic procedure B(iii) to give **8h** as an orange solid (819 mg, 85%). **^{1}H NMR** ($CDCl_3$) δ 2.73 (br s, 6H, CH_3NCH_3), 3.68 (s, 3H, azaindolyl-CH_3), 5.36 (d, 1H, *J* 12.5, CH=C*H*CO), 6.99 (dd, 1H, *J* 8.0 & 5.0, azaindolyl-H), 7.53 (d, 1H, *J* 12.5, C*H*=CHCO), 7.60 (s, 1H, azaindolyl-H), 8.16 (dd, 1H, *J* 4.5 & 1.5, azaindolyl-H), 8.49 (dd, 1H, *J* 8.0 & 1.5, azaindolyl-H). **HRMS** (ESI-TOF) *m/z* 230.1285 [M+H]$^+$; calcd. for $C_{13}H_{16}N_3O^+$ 230.1288 [M+H]$^+$.

(*E*)-3-(Dimethylamino)-1-(7-methyl-7*H*-pyrrolo[2,3-*b*]pyridin-3-yl)prop-2-en-1-one (8i)

4d (435 mg, 2.50 mmol) and DMF-DMA (1.00 mL, 7.53 mmol) were reacted according to general synthetic procedure B(iii) to give **8i** as a brown solid (486 mg, 85%). **^{1}H NMR** ($CDCl_3$) δ 2.77 (br s, 6H, CH_3NCH_3), 4.04 (s, 3H, azaindolyl-CH_3), 5.54 (d, 1H, *J* 12.0, CH=C*H*CO), 6.74 (app t, 1H, *J* 6.5, azaindolyl-H), 7.41 (d, 1H, *J* 6.0, azaindolyl-H), 7.49 (d, 1H, *J* 12.5, C*H*=CHCO), 8.18 (s, 1H, azaindolyl-H), 8.70 (d, 1H, *J* 7.0, azaindolyl-H). **HRMS** (ESI-TOF) *m/z* 230.1285 [M+H]$^+$; calcd. for $C_{13}H_{16}N_3O^+$ 230.1288 [M+H]$^+$.

(*E*)-3-(Dimethylamino)-1-(1*H*-indazol-3-yl)prop-2-en-1-one (8j)

7a (4.80 g, 30.0 mmol) and 1-*tert*-butoxy-*N*,*N*,*N*′,*N*′-tetramethylmethanediamine (12.4 mL, 60.0 mmol) were reacted according to general synthetic procedure B(iv) to give **8j** as a beige solid (5.82 g, 90%). **^{1}H NMR** (DMSO-d_6) δ 2.89 (s, 3H, CH_3), 3.14 (s, 3H, CH_3), 6.09 (d, 1H, *J* 12.5, CH=C*H*CO), 7.19–7.23 (m, 1H, indazole-H), 7.37 (ddd, 1H, *J* 8.0 & 7.0 & 1.0, indazole-H), 7.58 (d, 1H, *J* 8.5, indazole-H), 7.74 (d, 1H, *J* 12.5, C*H*=CHCO), 8.28 (d, 1H, *J* 8.0, indazole-H), 13.42 (br s, 1H, indazole-NH). **HRMS** (ESI-TOF) *m/z* 216.1136 [M+H]$^+$; calcd. for $C_{12}H_{14}N_3O^+$ 216.1131 [M+H]$^+$.

(*E*)-3-(Dimethylamino)-1-(1-methyl-1*H*-indazol-3-yl)prop-2-en-1-one (8k)

7a (1.61 g, 10.0 mmol) and DMF-DMA (13.3 mL, 100 mmol) were reacted according to general synthetic procedure B(iii) to give **8k** as a yellow solid (1.60 g, 70%). **^{1}H NMR** ($CDCl_3$) δ 2.87 (br s, 3H, C*H*$_3$NCH$_3$), 3.04 (br s, 3H, CH$_3$NC*H*$_3$), 4.03 (s, 3H, indazolyl-CH_3), 6.12 (d, 1H, *J* 12.5, CH=C*H*CO), 7.21 (ddd, 1H, *J* 8.0 & 6.0 & 1.5, indazolyl-H), 7.29–7.35 (m, 1H, indazolyl-H), 7.32 (d, 1H, *J* 6.5, indazolyl-H), 7.80 (d, 1H, *J* 12.5, C*H*=CHCO), 8.43 (d, 1H, *J* 8.5, indazolyl-H). **HRMS** (ESI-TOF) *m/z* 230.1291 [M+H]$^+$; calcd. for $C_{13}H_{16}N_3O^+$ 230.1288 [M+H]$^+$.

(*E*)-3-(Dimethylamino)-2-(1*H*-indazole-3-carbonyl)acrylonitrile (8l)

To DMF-DMA (2.00 mL, 15.0 mmol) was added to **7b** (352 mg, 1.90 mmol). The suspension was stirred at room temperature for 30 min, and concentrated *via* forced evaporation under a stream of N_2 and *in vacuo*. The residue was purified by FlashMaster Personal$^+$ chromatography (silica gel, DCM ramping to DCM:CH_3OH = 97:3) to give **8l** as a yellow solid (330 mg, 72%). **^{1}H NMR** (DMSO-d_6) δ 3.28 (s, 3H, CH_3), 3.39 (s, 3H, CH_3), 7.26 (app t, 1H, *J* 7.5, indazolyl-H), 7.42 (app t, 1H, *J* 7.5, indazolyl-H), 7.62 (d, 1H, *J* 8.5, indazolyl-H), 8.09 (d, 1H, *J* 8.0, indazolyl-H), 8.51 (s, 1H, CH=C(CN)CO), 13.69 (br s, 1H, indazolyl-NH). **HRMS** (ESI-TOF) *m/z* 503.1917 [2M+Na]$^+$; calcd. for $C_{26}H_{24}N_8NaO_2^+$ 503.1914 [2M+Na]$^+$.

1-(4-(4-Aminophenyl)piperazin-1-yl)ethan-1-one (10a)

1-(4-(4-Nitrophenyl)piperazin-1-yl)ethan-1-one (**9a**, 2.50 g, 10.0 mmol) was reduced according to general synthetic procedure C to give **10a** as a grey solid (2.19 g, 100%). **^{1}H NMR** ($CDCl_3$): δ 2.09 (s, 3H, CH_3), 2.92–2.94 (m, 4H, 2 × CH_2), 3.55–3.60 (m, 2H, CH_2), 3.73–3.78 (m, 2H, CH_2), 3.45 (br s, 2H, NH_2), 6.64 (d, 2H, *J* 9.0, 2 × Ph-H), 6.81 (d, 2H, *J* 9.0, 2 × Ph-H). **HRMS** (ESI-TOF) *m/z* 220.1452 [M+H]$^+$; calcd. For $C_{12}H_{18}N_3O^+$ 220.1444 [M+H]$^+$.

3-(4-Methylpiperazin-1-yl)aniline (10b)

1-Methyl-4-(3-nitrophenyl)piperazine (**9b**, 5.00 g, 22.6 mmol) was reduced according to general synthetic procedure C to give **10b** as an orange solid (4.32 g, 100%). **^{1}H NMR** ($CDCl_3$): δ 2.34 (s, 3H, CH_3), 2.55 (t, 4H, *J* 5.0, 2 × CH_2), 3.18 (t, 4H, *J* 5.0, 2 × CH_2), 3.60 (br s, 2H, NH_2), 6.21 (d, 1H, *J* 8.0, Ph-H), 6.25 (s, 1H, Ph-H), 6.37 (d, 1H, *J* 8.0, Ph-H), 7.06 (t, 1H, *J* 8.0, Ph-H). **HRMS** (ESI-TOF) *m/z* 192.1483 [M+H]$^+$; calcd. for $C_{11}H_{18}N_3^+$ 192.1495 [M+H]$^+$.

1-(4-(4-Acetylpiperazin-1-yl)phenyl)guanidine hydrochloride (11a)

Amine **10a** (1.50 g, 6.84 mmol) and cyanamide (580 mg, 13.7 mmol) were reacted using general synthetic procedure D to give **11a** as a grey solid (1.73 g, 85%). **^{1}H NMR** (D_2O) δ 2.17 (s, 3H, CH_3), 3.20 (t, 2H, *J* 5.0, CH_2), 3.26 (t, 2H, *J* 5.0, CH_2), 3.70–3.75 (m, 4H, 2 × CH_2), 7.01 (d, 2H, *J* 9.0, 2 × Ph-H), 7.63 (d, 2H, *J* 9.0, 2 × Ph-H) (five proton signals (NH_2 & 2 × NH & HCl) not observed due to H/D exchange). **HRMS** (ESI-TOF) *m/z* 262.1675 [M-HCl+H]$^+$; calcd. For $C_{13}H_{20}N_5O^+$ 262.1662 [M-HCl+H]$^+$.

1-(3-(4-Methylpiperazin-1-yl)phenyl)guanidine dihydrochloride (11b)

Amine **10b** (4.00 g, 20.9 mmol) and cyanamide (1.77 g, 41.8 mmol) were reacted using general synthetic procedure D to

give **11b** as a grey solid (5.35 g, 95%). **^{1}H NMR** (DMSO-d_6) δ 2.19 (s, 3H, CH_3), 2.42 (t, 4H, *J* 4.5, 2 × CH_2), 3.13 (t, 4H, *J* 4.5, 2 × CH_2), 6.58 (d, 1H, *J* 8.0, Ph-H), 6.68 (s, 1H, Ph-H), 6.84 (d, 1H, *J* 8.5, Ph-H), 7.01 (t, 1H, *J* 8.0, Ph-H) (six proton signals (NH_2 & 2 × NH & 2 × HCl) not observed due to H/D exchange). **HRMS** (ESI-TOF) *m/z* 234.1710 [M-2HCl+H]$^+$; calcd. For $C_{12}H_{20}N_5^+$ 234.1713 [M-2HCl+H]$^+$.

1-(4-(4-((4-(1*H*-Pyrrolo[2,3-*b*]pyridin-3-yl)pyrimidin-2-yl) amino)phenyl)piperazin-1-yl)ethan-1-one (12a)

Guanidine **11a** (522 mg, 2.00 mmol) and enaminone **8g** (216 mg, 1.00 mmol) were coupled using general synthetic procedure E. The residue was purified by FlashMaster Personal$^+$ chromatography (silica gel, DCM ramping to DCM:CH_3OH = 92:8) and washed with CH_3OH (15 mL) to give **12a** as a golden solid (230 mg, 56%). **m.p.** 148−150 °C (decomposed). **^{1}H NMR** (DMSO-d_6) δ 2.05 (s, 3H, CH_3), 3.04 (t, 2H, *J* 5.0, CH_2N(Ph)CH_2), 3.11 (t, 2H, *J* 5.0, CH_2N(Ph)CH_2), 3.59 (t, 2H, *J* 6.0, CH_2N($COCH_3$)CH_2), 3.61 (t, 2H, *J* 6.0, CH_2N($COCH_3$)CH_2), 6.98 (d, 2H, *J* 9.0, 2 × Ph-H), 7.25 (dd, 1H, *J* 8.0 & 5.0, azaindolyl-H), 7.44 (d, 2H, *J* 9.0, 2 × Ph-H), 7.62−7.66 (m, 3H, pyrimidinyl-H & 2 × azaindolyl-H), 8.46 (d, 1H, *J* 5.0), 8.67 (d, 1H, *J* 5.0) (total 2H, pyrimidinyl-H & azaindolyl-H), 9.42 (s, 1H, pyrimidinyl−NH−Ph), 13.63 (s, 1H, azaindolyl-NH). **^{13}C NMR** (DMSO-d_6) δ 21.3, 40.8, 45.6, 48.6, 49.3, 49.7, 106.9, 110.6, 116.6, 121.1, 121.8, 123.2, 126.6, 133.1, 141.3, 141.5, 146.2, 158.1, 160.4, 160.7, 168.3 (two carbon signals overlapping or obscured). **HRMS** (ESI-TOF) *m/z* 414.2041 [M+H]$^+$; calcd. for $C_{23}H_{24}N_7O^+$ 414.2037 [M+H]$^+$. **Anal. RP-HPLC**: t_R = 18.32 min, purity >98% (method A); t_R = 13.34 min, purity > 98% (method B).

1-(4-(4-((4-(1-Methyl-1*H*-pyrrolo[2,3-*b*]pyridin-3-yl)pyrimidin-2-yl)amino)phenyl)-piperazin-1-yl)ethan-1-one (12b)

Guanidine **11a** (522 mg, 2.00 mmol) and enaminone **8h** (230 mg, 1.01 mmol) were coupled using general synthetic procedure E. The residue was purified by FlashMaster Personal$^+$ chromatography (silica gel, DCM ramping to DCM:CH_3OH = 96:4) and washed with CH_3OH (15 mL) to give **12b** as a beige solid (245 mg, 57%). **m.p.** 218−220 °C. **^{1}H NMR** (DMSO-d_6) δ 2.05 (s, 3H, $COCH_3$), 3.03 (t, 2H, *J* 5.0, CH_2N(Ph)CH_2), 3.10 (t, 2H, *J* 5.0, CH_2N(Ph)CH_2), 3.59 (t, 2H, *J* 6.0, CH_2N($COCH_3$)CH_2), 3.60 (t, 2H, *J* 6.0, CH_2N($COCH_3$)CH_2), 3.90 (s, 3H, azaindolyl-CH_3), 6.96 (d, 2H, *J* 9.0, 2 × Ph-H), 7.16 (d, 1H, *J* 5.5, pyrimidinyl-H), 7.24 (dd, 1H, *J* 7.5 & 4.5, azaindolyl-H), 7.63 (d, 2H, *J* 9.0, 2 × Ph-H), 8.31 (d, 1H, *J* 5.5, pyrimidinyl-H), 8.36 (dd, 1H, *J* 4.5 & 1.0, azaindolyl-H), 8.48 (s, 1H, azaindolyl-H), 8.90 (apparent d, 1H, *J* 6.5, azaindolyl-H), 9.22 (s, 1H, pyrimidinyl−NH−Ph). **^{13}C NMR** (DMSO-d_6) δ 21.2, 31.4, 40.8, 45.7, 49.4, 49.8, 106.3, 111.2, 116.6, 117.1, 118.0, 120.8, 130.9, 132.5, 133.4, 143.4, 146.0, 148.2, 157.2, 160.3, 161.5, 168.3 (two carbon signals overlapping or obscured). **HRMS** (ESI-TOF) *m/z* 428.2198 [M+H]$^+$; calcd. for $C_{24}H_{26}N_7O^+$ 428.2193 [M+H]$^+$. **Anal. RP-HPLC**: t_R = 16.32 min, purity >95% (method A); t_R = 11.57 min, purity > 95% (method B).

N-(3-(4-methylpiperazin-1-yl)phenyl)-4-(1*H*-pyrrolo[2,3-*b*] pyridin-3-yl)pyrimidin-2-amine (12c)

Guanidine **11b** (233 mg, 1.00 mmol) and enaminone **8g** (108 mg, 500 μmol) were coupled using general synthetic procedure E. The residue was purified by glass column (silica gel, DCM ramping to DCM:CH_3OH = 95:5) and washed with EtOAc (10 mL) to give **12c** as a beige solid (33 mg, 17%). **m.p.** 228−230 °C (decomposed). **^{1}H NMR** (DMSO-d_6) δ 2.25 (s, 3H, CH_3), 3.13 (t, 4H, *J* = 4.5, CH_2N(Ph)CH_2), 6.58 (d, 1H, *J* = 8.0, Ph-H), 7.14 (t, 1H, *J* = 8.0, Ph-H), 7.19 (dd, 1H, *J* = 8.0 & 4.5, azaindolyl-H), 7.28−7.31 (m, 2H, pyrimidinyl-H & Ph-H), 7.41 (s, 1H, Ph-H), 8.31 (dd, 1H, *J* = 4.5 & 1.5, azaindolyl-H), 8.35 (d, 1H, *J* = 5.5, pyrimidinyl-H), 8.45 (d, 1H, *J* = 3.0, azaindolyl-H), 8.94 (s, 1H, azaindolyl-H), 9.27 (s, 1H, pyrimidinyl−NH−Ph), 12.31 (s, 1H, azaindolyl-NH) (four proton signals (CH_2N(CH_3) CH_2) not observed). **^{13}C NMR** (DMSO-d_6) δ 45.7, 48.2, 54.6, 106.5, 107.0, 109.0, 110.4, 112.4, 116.9, 117.6, 128.8, 129.1, 130.7, 141.5, 143.6, 149.3, 151.4, 157.1, 161.9, 167.4 (two carbon signals overlapping or obscured). **HRMS** (ESI-TOF) *m/z* 386.2081 [M+H]$^+$; calcd. for $C_{22}H_{24}N_7^+$ 386.2088 [M+H]$^+$. **Anal. RP-HPLC**: t_R = 13.42 min, purity >95% (method A); t_R = 9.82 min, purity > 95% (method B).

4-(1-Methyl-1*H*-pyrrolo[2,3-*b*]pyridin-3-yl)-*N*-(3-(4-methylpiperazin-1-yl)phenyl)pyrimidin -2-amine (12d)

Guanidine **11b** (233 mg, 1.00 mmol) and enaminone **8h** (115 mg, 500 μmol) were coupled using general synthetic procedure E. The residue was purified by glass column (silica gel, DCM ramping to DCM:CH_3OH = 96:4) and washed with EtOAc (10 mL) to give **12d** as a beige solid (63 mg, 32%). **m.p.** 192−194 °C (decomposed). **^{1}H NMR** (DMSO-d_6) δ 2.22 (s, 3H, piperazinyl-CH_3), 2.44 (t, 4H, *J* = 5.0, CH_2N(CH_3)CH_2), 3.12 (t, 4H, *J* = 5.0, CH_2N(Ph)CH_2), 3.91 (s, 3H, azaindolyl-CH_3), 6.58 (d, 1H, *J* = 8.0, Ph-H), 7.14 (t, 1H, *J* = 8.0, Ph-H), 7.21 (d, 1H, *J* = 5.0, pyrimidinyl-H), 7.24 (dd, 1H, *J* = 8.0 & 4.5, azaindolyl-H), 7.29 (d, 1H, *J* = 8.0, Ph-H), 7.40 (s, 1H, Ph-H), 8.35−8.38 (m, 2H, azaindolyl-H & pyrimidinyl-H), 8.50 (s, 1H, azaindolyl-H), 8.94 (d, 1H, *J* = 7.5, azaindolyl-H), 9.28 (s, 1H, pyrimidinyl−NH−Ph). **^{13}C NMR** (DMSO-d_6) δ 31.4, 45.7, 48.2, 54.6, 106.8, 109.0, 110.4, 111.1, 117.1, 117.9, 128.8, 130.9, 132.6, 141.4, 143.5, 148.2, 151.4, 157.2, 160.2, 161.5, 167.0 (two carbon signals overlapping or obscured). **HRMS** (ESI-TOF) *m/z* 400.2243 [M+H]$^+$; calcd. for $C_{23}H_{26}N_7^+$ 400.2244 [M+H]$^+$. **Anal. RP-HPLC**: t_R = 14.01 min, purity >96% (method A); t_R = 10.33 min, purity > 96% (method B).

1-(4-(3-((4-(1*H*-Pyrrolo[2,3-*b*]pyridin-3-yl)pyrimidin-2-yl) amino)phenyl)-1,4-diazepan-1-yl)ethan-1-one (12e)

Guanidine **11c** (300 mg, 1.08 mmol) and enaminone **8g** (110 mg, 510 μmol) were coupled using general synthetic procedure E. The residue was purified by FlashMaster Personal$^+$ chromatography (silica gel, DCM ramping to DCM:CH_3OH = 91:9 + 0.2% NH_3 (32% in H_2O)) and washed with CH_3OH (10 mL) to give **12e** as a beige solid (65 mg, 30%). **m.p.** 150−152 °C. **^{1}H NMR** (DMSO-d_6) (**12e** exists as two rotamers in approximately 1:1 ratio.) δ 1.79−1.83 (m, 1H, $CH_2CH_2CH_2$ of one rotamer), 1.87 (s, 1.5H, CH_3 of one rotamer), 1.89−1.93 (m, 1H, $CH_2CH_2CH_2$ of the other rotamer), 1.99 (s, 1.5H, CH_3 of the other rotamer), 3.29 (t, 2H, *J* 6.0), 3.50 (t, 2H, *J* 6.0), 3.53 (t, 1H, *J* 6.0), 3.59−3.63 (m, 2H), 3.64 (t, 1H, *J* 5.0) (total 8H, CH_2N($COCH_3$)CH_2 & CH_2N(Ph)CH_2), 6.39 (d, 1H, *J* 8.0, Ph-H), 7.09 (t, 1H, *J* 8.0, Ph-H), 7.15 (d, 1H, *J* 8.0, Ph-H), 7.18−7.27 (m, 2H, Ph-H & azaindolyl-H), 7.29 (d, 1H, *J* 5.5, pyrimidinyl-H), 8.31 (dd, 1H, *J* 4.5 & 1.5, azaindolyl-H), 8.34 (d, 1H, *J* 5.5, pyrimidinyl-H), 8.45 (s, 1H, azaindolyl-H), 8.97 (d, 1H, *J* 7.5, azaindolyl-H), 9.21 (s, 1H, pyrimidinyl−NH−Ph), 12.30 (s, 1H, azaindolyl-NH). **^{13}C NMR** (DMSO-d_6) δ 21.0, 21.3 (one carbon), 24.0, 25.9 (one carbon), 43.9, 44.5, 46.9, 47.0, 47.1, 48.2, 49.0, 49.7 (four carbons), 102.5, 102.7 (one carbon), 105.3, 105.4 (one carbon), 106.9, 107.4, 112.4, 116.9, 117.7, 129.1, 129.2 (one carbon), 130.7, 141.9, 143.6, 147.3, 147.5, 149.3, 157.0, 160.2, 161.9, 169.0, 169.3 (one carbon). **HRMS** (ESI-TOF) *m/z* 428.2194 [M+H]$^+$; calcd. for $C_{24}H_{26}N_7O^+$ 428.2193 [M+H]$^+$. **Anal. RP-HPLC**: t_R = 16.74 min, purity >96% (method A); t_R = 11.76 min, purity > 95% (method B).

1-(4-(3-((4-(7-Methyl-7*H*-pyrrolo[2,3-*b*]pyridin-3-yl)pyrimidin-2-yl)amino)phenyl)-1,4-diazepan-1-yl)ethan-1-one (12f)

Guanidine **11c** (300 mg, 1.08 mmol) and enaminone **8i** (115 mg, 500 μmol) were coupled using general synthetic procedure E. The residue was purified by FlashMaster Personal$^+$ chromatography (silica gel, DCM ramping to DCM:CH_3OH = 97:3 + 0.2% NH_3 (32% in H_2O)) and washed with Et_2O (10 mL) to give **12f** as a yellow solid (56 mg, 25%). **m.p.** 144−146 °C. **^{1}H NMR** (DMSO-d_6) (**12f** exists as two rotamers in approximately 1:1 ratio.) δ 1.79−1.83 (m, 1H, $CH_2CH_2CH_2$ of one rotamer), 1.87 (s, 1.5H, CH_3 of one rotamer), 1.89−1.93 (m, 1H, $CH_2CH_2CH_2$ of the other rotamer), 1.99 (s, 1.5H, CH_3 of the other rotamer), 3.30 (t, 2H, *J* 6.0), 3.50 (t, 2H, *J* 5.5), 3.53 (t, 1H, *J* 5.5), 3.60−3.64 (m, 2H), 3.65 (t, 1H, *J* 5.0) (total 8H, CH_2N($COCH_3$)CH_2 & CH_2N(Ph)CH_2), 4.31 (s, 3H, azaindolyl-CH_3),

6.38 (d, 1H, *J* 8.0, Ph-H), 7.08 (t, 1H, *J* 8.0, Ph-H), 7.14–7.23 (m, 3H, Ph-H & azaindolyl-H & pyrimidinyl-H), 7.24 (d, 1H, *J* 8.0, Ph-H), 8.25 (d, 1H, *J* 5.5, pyrimidinyl-H), 8.26 (d, 1H, *J* 5.5, azaindolyl-H), 8.54 (s, 1H, azaindolyl-H), 9.09 (s, 1H, pyrimidinyl–NH–pyridinyl), 9.19 (d, 1H, *J* 7.5, azaindolyl-H). **^{13}C NMR** (DMSO-d_6) δ 21.0, 21.3 (one carbon), 24.0, 25.9 (one carbon), 43.9, 44.5, 46.9, 47.0, 47.1, 48.2, 49.1, 49.7 (four carbons), 102.4, 102.6 (one carbon), 105.0, 105.1 (one carbon), 106.4, 107.3, 111.6, 113.5, 126.4, 129.1, 133.1, 134.3, 142.1, 147.2, 147.4, 147.5 (one carbon), 150.7, 156.5, 160.2, 162.2, 169.0, 169.3 (one carbon) (one carbon signal overlapping or obscured). **HRMS** (ESI-TOF) *m/z* 442.2353 $[M+H]^+$; calcd. for $C_{25}H_{28}N_7O^+$ 442.2350 $[M+H]^+$. **Anal. RP-HPLC**: t_R = 13.68 min, purity >98% (method A); t_R = 10.18 min, purity > 98% (method B).

1-(4-(4-((4-(1*H*-Pyrrolo[3,2-*b*]pyridin-3-yl)pyrimidin-2-yl) amino)phenyl)piperazin-1-yl)ethan-1-one (12g)

Guanidine **11a** (523 mg, 2.01 mmol) and enaminone **8f** (220 mg, 1.02 mmol) were coupled using general synthetic procedure. The residue was purified by FlashMaster Personal$^+$ chromatography (silica gel, DCM ramping to DCM:CH_3OH = 95:5) and washed with CH_3OH (10 mL) to give **12g** as a yellow solid (213 mg, 51%). **m.p.** 293–295 °C (decomposed). **^{1}H NMR** (DMSO-d_6) δ 2.04 (s, 3H, CH_3), 3.01 (t, 2H, *J* 5.0, CH_2N(Ph)CH_2), 3.07 (t, 2H, *J* 5.0, CH_2N(Ph)CH_2), 3.57 (t, 2H, *J* 6.0, CH_2N(COCH$_3$)CH_2), 3.59 (t, 2H, *J* 6.0, CH_2N(COCH$_3$)CH_2), 6.96 (d, 2H, *J* 9.0, 2 × Ph-H), 7.24 (dd, 1H, *J* 8.0 & 4.5, azaindolyl-H), 7.73 (d, 2H, *J* 9.0, 2 × Ph-H), 7.92 (dd, 1H, *J* 8.0 & 1.5, azaindolyl-H), 8.15 (d, 1H, *J* 5.0, pyrimidinyl-H), 8.39 (s, 1H, azaindolyl-H), 8.41 (d, 1H, *J* 5.0, pyrimidinyl-H), 8.51 (dd, 1H, *J* 4.5 & 1.5, azaindolyl-H), 9.19 (s, 1H, pyrimidinyl–NH–Ph), 11.93 (s, 1H, azaindolyl-NH). **^{13}C NMR** (DMSO-d_6) δ 21.2, 40.8, 45.7, 49.4, 49.9, 108.4, 113.3, 116.8, 117.2, 119.8, 119.9, 130.0, 130.7, 133.9, 143.6, 143.7, 145.5, 158.0, 159.9, 160.1, 168.3 (two carbon signals overlapping or obscured). **HRMS** (ESI-TOF) *m/z* 414.2049 $[M+H]^+$; calcd. for $C_{23}H_{24}N_7O^+$ 414.2037 $[M+H]^+$. **Anal. RP-HPLC**: t_R = 13.57 min, purity >98% (method A); t_R = 9.78 min, purity > 98% (method B).

N-(3-(4-methylpiperazin-1-yl)phenyl)-4-(1*H*-pyrrolo[3,2-*b*] pyridin-3-yl)pyrimidin-2-amine (12h)

Guanidine **11b** (233 mg, 1.00 mmol) and enaminone **8f** (108 mg, 500 μmol) were coupled using general synthetic procedure E. The residue was purified by glass column (silica gel, DCM ramping to DCM:CH_3OH = 94:6) and washed with EtOAc (10 mL) to give **12h** as a beige solid (74 mg, 38%). **m.p.** 222–224 °C (decomposed). **^{1}H NMR** (DMSO-d_6) δ 2.25 (s, 3H, CH_3), 3.16 (t, 4H, *J* = 5.0, $CH_2N(Ph)CH_2$), 6.54 (d, 1H, *J* = 8.0, Ph-H), 7.13 (t, 1H, *J* = 8.0, Ph-H), 7.25 (dd, 1H, *J* = 8.0 & 4.5, azaindolyl-H), 7.30 (d, 1H, *J* = 8.0, Ph-H), 7.60 (s, 1H, Ph-H), 7.93 (dd, 1H, *J* = 4.5 & 1.5, azaindolyl-H), 8.19 (d, 1H, *J* = 5.0, pyrimidinyl-H), 8.38 (s, 1H, azaindolyl-H), 8.46 (d, 1H, *J* = 5.0, pyrimidinyl-H), 8.52 (dd, 1H, *J* = 4.5 & 1.5, azaindolyl-H), 9.24 (s, 1H, pyrimidinyl–NH–Ph), 12.02 (s, 1H, azaindolyl-NH) (four proton signals (CH_2N(CH$_3$) CH_2) not observed). **^{13}C NMR** (DMSO-d_6) δ 45.8, 48.4, 54.7, 105.9, 108.7, 109.8, 113.3, 117.3, 119.8, 128.9, 130.0, 130.5, 141.8, 143.6, 143.7, 151.4, 158.1, 159.9, 160.1, 167.5 (two carbon signals overlapping or obscured). **HRMS** (ESI-TOF) *m/z* 386.2072 $[M+H]^+$; calcd. for $C_{22}H_{24}N_7^+$ 386.2088 $[M+H]^+$. **Anal. RP-HPLC**: t_R = 10.96 min, purity >95% (method A); t_R = 8.81 min, purity > 95% (method B).

1-(4-(3-((4-(1*H*-Pyrrolo[3,2-*b*]pyridin-3-yl)pyrimidin-2-yl) amino)phenyl)-1,4-diazepan-1-yl)ethan-1-one (12i)

Guanidine **11c** (300 mg, 1.08 mmol) and enaminone **8f** (110 mg, 0.510 mmol) were coupled using general synthetic procedure E. The residue was purified by FlashMaster Personal$^+$ chromatography (silica gel, DCM ramping to DCM:CH_3OH = 95:5 + 0.2% NH_3 (32% in H_2O)) and washed with CH_3OH (10 mL) to give **12i** as a beige solid (71 mg, 33%). **m.p.** 155–157 °C. **^{1}H NMR** (DMSO-d_6) (**12i** exists as two rotamers in approximately 1:1 ratio.) δ 1.82–1.86 (m, 1H, $CH_2CH_2CH_2$ of one rotamer), 1.88 (s, 1.5H, CH_3 of one rotamer), 1.91–1.95 (m, 1H, $CH_2CH_2CH_2$ of the other rotamer), 2.00 (s, 1.5H, CH_3 of the other rotamer), 3.29 (t, 2H, *J* 5.5), 3.52 (t, 2H, *J* 5.5), 3.56 (t, 1H, *J* 5.5), 3.60–3.64 (m, 2H), 3.66 (t, 1H, *J* 5.0) (total 8H, $CH_2N(COCH_3)CH_2$ & $CH_2N(Ph)CH_2$), 6.37 (d, 1H, *J* 8.0, Ph-H), 7.09 (t, 1H, *J* 8.0, Ph-H), 7.21–7.23 (m, 1H, Ph-H), 7.24 (dd, 1H, *J* 8.0 & 4.5, azaindolyl-H), 7.30–7.32 (m, 1H, Ph-H), 7.92 (dd, 1H, *J* 8.0 & 1.5, azaindolyl-H), 8.18 (d, 1H, *J* 5.0, pyrimidinyl-H), 8.38 (dd, 1H, *J* 4.5 & 1.5, azaindolyl-H), 8.45 (s, 1H, azaindolyl-H), 8.51 (d, 1H, *J* 5.0, pyrimidinyl-H), 9.15 (s, 1H, pyrimidinyl–NH–Ph), 11.98 (s, 1H, azaindolyl-NH). **^{13}C NMR** (DMSO-d_6) δ 21.0, 21.3 (one carbon), 24.1, 26.0 (one carbon), 44.0, 44.6, 46.9, 47.0, 47.1, 48.3, 48.9, 49.7 (four carbons), 102.0, 102.1 (one carbon), 104.9, 105.0 (one carbon), 107.0, 108.7, 113.3, 117.2, 119.8, 129.3, 129.9, 130.5, 142.1, 143.6, 147.2, 147.6, 158.0, 159.9, 160.0, 160.1 (one carbon), 169.1, 169.3 (one carbon). **HRMS** (ESI-TOF) *m/z* 428.2206 $[M+H]^+$; calcd. for $C_{24}H_{26}N_7O^+$ 428.2193 $[M+H]^+$. **Anal. RP-HPLC**: t_R = 15.21 min, purity >95% (method A); t_R = 10.93 min, purity > 95% (method B).

1-(4-(4-((4-(1*H*-Indol-3-yl)pyrimidin-2-yl)amino)phenyl) piperazin-1-yl)ethan-1-one (12j) & 1-(4-(4-((4-(1-Tosyl-1*H*-indol-3-yl)pyrimidin-2-yl)amino)phenyl)piperazin-1-yl)ethan-1-one (12l)

Guanidine **11a** (522 mg, 2.00 mmol) and enaminone **8e** (368 mg, 1.00 mmol) were coupled using general synthetic procedure E. The residue was purified by glass column chromatography (silica gel, DCM ramping to DCM:CH_3OH = 99:1 for **12l**, and ramping to DCM:CH_3OH = 96:4 for **12j**) and washed with CH_3OH (15 mL) to give **12l** as a beige solid (78 mg, 14%) and **12j** (185 mg, 45%) as a white solid.

12j: **m.p.** 250–252 °C (decomposed). **^{1}H NMR** (DMSO-d_6) δ 2.05 (s, 3H, CH_3), 3.03 (t, 2H, *J* = 5.0, CH_2N(Ph)CH_2), 3.09 (t, 2H, *J* = 5.0, CH_2N(Ph)CH_2), 3.57–3.61 (m, 4H, CH_2N(COCH$_3$)CH_2), 6.95 (d, 2H, *J* = 9.0, 2 × Ph-H), 7.13 (t, 1H, *J* = 7.5, indolyl-H), 7.17–7.21 (m, 2H, indolyl-H & pyrimidinyl-H), 7.46 (d, 1H, *J* = 8.0, indolyl-H), 7.67 (d, 2H, *J* = 9.0, 2 × Ph-H), 8.26–8.29 (m, 2H, pyrimidinyl-H & indolyl-H), 8.58 (br s, 1H, pyrimidinyl–NH–Ph), 9.16 (s, 1H, indolyl-H), 11.75 (s, 1H, indolyl-NH). **^{13}C NMR** (DMSO-d_6) δ 21.2, 40.1, 40.8, 45.6, 49.4, 49.8, 106.8, 111.9, 113.7, 116.6, 120.5, 120.6, 122.1, 122.4, 125.2, 128.8, 133.7, 137.1, 145.8, 156.7, 160.3, 162.5, 168.2 (one carbon signal overlapping or obscured). **HRMS** (ESI-TOF) *m/z* 413.2099 $[M+H]^+$; calcd. for $C_{24}H_{25}N_6O^+$ 413.2084 $[M+H]^+$. **Anal. RP-HPLC**: t_R = 15.81 min, purity >96% (method A); t_R = 11.82 min, purity > 95% (method B).

12l: **m.p.** 229–231 °C (decomposed). **^{1}H NMR** (DMSO-d_6) δ 2.04 (s, 3H, $COCH_3$), 2.32 (s, 3H, tosyl-CH_3), 3.02 (t, 2H, *J* = 5.0, CH_2N(Ph) CH_2), 3.09 (t, 2H, *J* = 5.0, $CH_2N(Ph)CH_2$), 3.55–3.61 (m, 4H, CH_2N(COCH$_3$)CH_2), 6.94 (d, 2H, *J* = 9.0, 2 × Ph-H), 7.32 (t, 1H, *J* = 7.5, indolyl-H), 7.39–7.46 (m, 4H, pyrimidinyl-H, indolyl-H & 2 × tosyl-H), 7.60 (d, 2H, *J* = 9.0, 2 × Ph-H), 7.95–8.01 (m, 3H, indolyl-H & 2 × tosyl-H), 8.42 (d, 1H, *J* = 5.0, pyrimidinyl-H), 8.63 (br s, 1H, pyrimidinyl–NH–Ph), 8.72 (s, 1H, indolyl-H), 9.37 (s, 1H, indolyl-H). **^{13}C NMR** (DMSO-d_6) δ 21.2, 21.3, 40.2, 40.8, 45.6, 49.2, 49.7, 108.1, 113.1, 116.5, 120.0, 121.0, 123.6, 124.0, 125.4, 127.0, 127.7, 128.5, 130.4, 133.0, 133.8, 134.8, 146.0, 146.2, 158.0, 160.1, 160.3, 168.2 (three carbon signals overlapping or obscured). **HRMS** (ESI-TOF) *m/z* 567.2177 $[M+H]^+$; calcd. for $C_{31}H_{31}N_6O_3S^+$ 567.2173 $[M+H]^+$. **Anal. RP-HPLC**: t_R = 22.53 min, purity >97% (method A); t_R = 18.86 min, purity > 98% (method B).

1-(4-(4-((4-(1-Methyl-1*H*-indol-3-yl)pyrimidin-2-yl)amino) phenyl)piperazin-1-yl)ethan-1-one (12k)

Guanidine **11a** (522 mg, 2.00 mmol) and enaminone **8d** (228 mg, 1.00 mmol) were coupled using general synthetic procedure E. The residue was purified by glass column chromatography (silica gel, DCM ramping to DCM:CH_3OH = 97:3) and washed with EtOAc (20 mL) to give **12k** as a beige solid (273 mg, 64%). **m.p.** 228–230 °C. **^{1}H NMR** (DMSO-d_6) δ 2.05 (s, 3H, $COCH_3$), 3.03 (t, 2H,

J = 5.0, CH_2N(Ph)CH_2), 3.09 (t, 2H, J = 5.0, CH_2N(Ph)CH_2), 3.57–3.61 (m, 4H, CH_2N(COCH_3)CH_2), 3.88 (s, 3H, indolyl-CH_3), 6.95 (d, 2H, J = 9.0, 2 × Ph-H), 7.12 (d, 1H, J = 5.5, pyrimidinyl-H), 7.18 (t, 1H, J = 7.5, indolyl-H), 7.26 (t, 1H, J = 7.5, indolyl-H), 7.52 (d, 1H, J = 8.0, indolyl-H), 7.67 (d, 2H, J = 9.0, 2 × Ph-H), 8.27–8.28 (m, 2H, pyrimidinyl-H & indolyl-H), 8.60 (br s, 1H, pyrimidinyl–NH–Ph), 9.17 (s, 1H, indolyl-H). **^{13}C NMR** (DMSO-d_6) δ 21.2, 33.0, 40.8, 45.6, 49.4, 49.8, 106.6, 110.3, 112.6, 116.6, 120.6, 120.7, 122.2, 122.5, 125.6, 132.7, 133.6, 137.6, 145.8, 156.8, 160.3, 162.0, 168.2 (two carbon signals overlapping or obscured). **HRMS** (ESI-TOF) m/z 427.2232 $[M+H]^+$; calcd. for $C_{25}H_{27}N_6O^+$ 427.2241 $[M+H]^+$. **Anal. RP-HPLC**: t_R = 16.93 min, purity >98% (method A); t_R = 12.58 min, purity > 99% (method B).

2-((4-(4-Acetylpiperazin-1-yl)phenyl)amino)-4-(1*H*-indol-3-yl) pyrimidine-5-carbonitrile (12m)

Guanidine **11a** (261 mg, 1.00 mmol) and enaminone **8a** (120 mg, 500 μmol) were coupled using general synthetic procedure E. The residue was purified by glass column chromatography (silica gel, DCM ramping to DCM:CH_3OH = 98:2) and washed with CH_3OH (15 mL) to give **12m** as a beige solid (62 mg, 28%). **m.p.** 278–280 °C (decomposed). **^{1}H NMR** (DMSO-d_6) δ 2.05 (s, 3H, CH_3), 3.08 (t, 2H, J = 5.0, CH_2N(Ph)CH_2), 3.14 (t, 2H, J = 5.0, CH_2N(Ph)CH_2), 3.58–3.60 (m, 4H, CH_2N(COCH_3)CH_2), 6.99 (d, 2H, J = 9.0, 2 × Ph-H), 7.23–7.25 (m, 2H, 2 × indolyl-H), 7.53 (d, 1H, J = 8.5, indolyl-H), 7.57–7.59 (m, 2H, 2 × Ph-H), 8.51–8.53 (m, 1H, indolyl-H), 8.73 (s, 1H, pyrimidinyl-H), 10.01 (s, 1H, indolyl-H), 12.03 (s, 1H, indolyl-NH) (one proton signal (pyrimidinyl–NH–Ph) not observed). **^{13}C NMR** (DMSO-d_6) δ 21.2, 40.2, 40.7, 45.5, 48.9, 49.3, 108.2, 112.1, 116.2, 120.0, 121.2, 122.9, 123.1, 123.5, 130.5, 136.4, 140.8, 163.1, 168.3 (six carbon signals overlapping or obscured). **HRMS** (ESI-TOF) m/z 438.2031 $[M+H]^+$; calcd. for $C_{25}H_{24}N_7O^+$ 438.2037 $[M+H]^+$. **Anal. RP-HPLC**: t_R = 19.80 min, purity >95% (method A); t_R = 15.81 min, purity > 95% (method B).

2-((4-(4-Acetylpiperazin-1-yl)phenyl)amino)-4-(1-methyl-1*H*-indol-3-yl)pyrimidine-5-carbonitrile (12n)

Guanidine **11a** (261 mg, 1.00 mmol) and enaminone **8b** (127 mg, 500 μmol) were coupled using general synthetic procedure E. The residue was purified by glass column (silica gel, DCM ramping to DCM:CH_3OH = 99:1) and washed with CH_3OH (15 mL) to give **12n** as a white solid (60 mg, 27%). **m.p.** 213–215 °C (decomposed). **^{1}H NMR** (DMSO-d_6) δ 2.05 (s, 3H, $COCH_3$), 3.08 (t, 2H, J = 5.0, CH_2N(Ph)CH_2), 3.14 (t, 2H, J = 5.0, CH_2N(Ph)CH_2), 3.59–3.60 (m, 4H, CH_2N(COCH_3)CH_2), 3.94 (s, 3H, indolyl-CH_3), 6.99 (d, 2H, J = 9.0, 2 × Ph-H), 7.30–7.32 (m, 2H, 2 × indolyl-H), 7.56–7.58 (m, 3H, indolyl-H & 2 × Ph-H), 8.47–8.49 (m, 1H, indolyl-H), 8.72 (s, 1H, pyrimidinyl-H), 10.01 (s, 1H, indolyl-H) (one proton signal (pyrimidinyl–NH–Ph) not observed). **^{13}C NMR** (DMSO-d_6) δ 21.2, 33.4, 40.1, 40.7, 45.5, 48.9, 49.3, 110.5, 116.2, 119.4, 121.5, 123.0, 126.0, 132.5, 134.0, 137.1, 160.2, 161.1, 163.3, 168.3 (six carbon signals overlapping or obscured). **HRMS** (ESI-TOF) m/z 452.2179 $[M+H]^+$; calcd. for $C_{26}H_{26}N_7O^+$ 452.2193 $[M+H]^+$. **Anal. RP-HPLC**: t_R = 20.97 min, purity >99% (method A); t_R = 17.13 min, purity > 98% (method B).

2-((4-(4-Acetylpiperazin-1-yl)phenyl)amino)-4-(2-methyl-1*H*-indol-3-yl)pyrimidine-5-carbonitrile (12o)

Guanidine **11a** (261 mg, 1.00 mmol) and enaminone **8c** (127 mg, 0.50 mmol) were coupled using general synthetic procedure E. The residue was purified by glass column chromatography (silica gel, DCM ramping to DCM:CH_3OH = 98:2) and washed with CH_3OH (10 mL) to give **12o** as a yellow solid (30 mg, 13%). **m.p.** 208–210 °C (decomposed). **^{1}H NMR** (DMSO-d_6) δ 2.03 (s, 3H, $COCH_3$), 2.55 (s, 3H, indolyl-CH_3), 3.02 (t, 2H, J = 5.0, CH_2N(Ph)CH_2), 3.09 (t, 2H, J = 5.0, CH_2N(Ph)CH_2), 3.55–3.56 (m, 4H, CH_2N(COCH_3)CH_2), 6.91–6.93 (m, 2H, 2 × Ph-H), 7.08 (t, 1H, J = 7.5, indolyl-H), 7.13 (t, 1H, J = 7.5, indolyl-H), 7.39 (d, 1H, J = 8.0, indolyl-H), 7.62–7.64 (m, 3H, indolyl-H & 2 × Ph-H), 8.82 (s, 1H, pyrimidinyl-H), 10.13 (s, 1H, pyrimidinyl–NH–Ph), 11.74 (s, 1H, indolyl-NH). **^{13}C NMR** (DMSO-d_6) δ 13.8, 21.3, 40.3, 40.8, 45.6, 48.9, 49.3, 111.2, 114.7, 116.3, 118.3, 120.2, 121.8, 126.4, 131.5, 135.3, 147.1, 159.9, 165.0, 165.9, 168.5 (five carbon signals overlapping or obscured). **HRMS** (ESI-TOF) m/z 452.2185 $[M+H]^+$; calcd. for $C_{26}H_{26}N_7O^+$ 452.2193 $[M+H]^+$. **Anal. RP-HPLC**: t_R = 19.24 min, purity >95% (method A); t_R = 15.64 min, purity > 96% (method B).

1-(4-(4-((4-(1*H*-Indazol-3-yl)pyrimidin-2-yl)amino)phenyl) piperazin-1-yl)ethan-1-one (12p)

Guanidine **11a** (522 mg, 2.00 mmol) and enaminone **8j** (215 mg, 1.00 mmol) were coupled using general synthetic procedure E. The residue was purified by glass column chromatography (silica gel, DCM ramping to DCM:CH_3OH = 97:3) and washed with EtOAc (20 mL) and CH_3OH (5 mL) to give **12p** as a yellow solid (248 mg, 60%). **m.p.** 275–277 °C (decomposed). **^{1}H NMR** (DMSO-d_6) δ 2.04 (s, 3H, CH_3), 3.02 (t, 2H, J = 5.0, CH_2N(Ph)CH_2), 3.09 (t, 2H, J = 5.0, CH_2N(Ph)CH_2), 3.58–3.59 (m, 4H, CH_2N(COCH_3)CH_2), 6.95 (d, 2H, J = 9.0, 2 × Ph-H), 7.43 (d, 1H, J = 5.0, pyrimidinyl-H), 7.49 (t, 1H, J = 7.5, indazolyl-H), 7.67 (d, 2H, J = 9.0, 2 × Ph-H), 7.72 (d, 1H, J = 8.0, indazolyl-H), 7.85 (d, 1H, J = 7.5, indazolyl-H), 8.52 (d, 1H, J = 5.0, pyrimidinyl-H), 8.85 (br s, 1H, pyrimidinyl–NH–Ph), 9.49 (s, 1H, indazolyl-H), 13.26 (s, 1H, indazolyl-NH). **^{13}C NMR** (DMSO-d_6) δ 21.2, 40.8, 45.6, 49.2, 49.7, 108.4, 112.9, 116.6, 120.2, 120.4, 120.7, 125.8, 130.0, 133.2, 135.0, 140.8, 146.1, 158.6, 160.5, 164.1, 168.2 (two carbon signals overlapping or obscured). **HRMS** (ESI-TOF) m/z 414.2041 $[M+H]^+$; calcd. for $C_{23}H_{24}N_7O^+$ 414.2037 $[M+H]^+$. **Anal. RP-HPLC**: t_R = 18.51 min, purity >96% (method A); t_R = 13.44 min, purity > 97% (method B).

1-(4-(4-((4-(1-Methyl-1*H*-indazol-3-yl)pyrimidin-2-yl)amino) phenyl)piperazin-1-yl)ethan-1-one (12q)

Guanidine **11a** (522 mg, 2.00 mmol) and enaminone **8k** (230 mg, 1.00 mmol) were coupled using general synthetic procedure E. The residue was purified by glass column chromatography (silica gel, DCM ramping to DCM:CH_3OH = 98:2) and washed with CH_3OH (15 mL) to give **12q** as a yellow solid (154 mg, 36%). **m.p.** 268–270 °C (decomposed). **^{1}H NMR** (DMSO-d_6) δ 2.05 (s, 3H, $COCH_3$), 3.04 (t, 2H, J = 5.0, CH_2N(Ph)CH_2), 3.11 (t, 2H, J = 5.0, CH_2N(Ph)CH_2), 3.58–3.61 (m, 4H, CH_2N(COCH_3)CH_2), 4.17 (s, 3H, indazolyl-CH_3), 6.95 (d, 2H, J = 9.0, 2 × Ph-H), 7.28 (t, 1H, J = 7.5, indazolyl-H), 7.39 (d, 1H, J = 5.0, pyrimidinyl-H), 7.49 (t, 1H, J = 7.5, indazolyl-H), 7.65 (d, 2H, J = 9.0, 2 × Ph-H), 7.74 (d, 1H, J = 8.5, indazolyl-H), 8.45 (d, 1H, J = 5.0, pyrimidinyl-H), 8.67 (br s, 1H, pyrimidinyl–NH–Ph), 9.41 (s, 1H, indazolyl-H). **^{13}C NMR** (DMSO-d_6) δ 21.2, 36.0, 40.8, 45.6, 49.3, 49.7, 54.9, 106.7, 110.3, 116.5, 121.0, 121.7, 122.0, 123.3, 126.6, 133.1, 139.8, 141.3, 146.2, 158.1, 160.2, 160.4, 168.2 (one carbon signal overlapping or obscured). **HRMS** (ESI-TOF) m/z 428.2198 $[M+H]^+$; calcd. for $C_{24}H_{26}N_7O^+$ 428.2193 $[M+H]^+$. **Anal. RP-HPLC**: t_R = 20.10 min, purity >99% (method A); t_R = 15.17 min, purity > 99% (method B).

2-((4-(4-Acetylpiperazin-1-yl)phenyl)amino)-4-(1*H*-indazol-3-yl)pyrimidine-5-carbonitrile (12r)

Guanidine **11a** (522 mg, 2.00 mmol) and enaminone **8l** (240 mg, 1.00 mmol) were coupled using general synthetic procedure E. The residue was purified by glass column (silica gel, DCM ramping to DCM:CH_3OH = 98:2) and washed with CH_3OH (15 mL) to give **12r** as a yellow solid (136 mg, 31%). **m.p.** > 300 °C. **^{1}H NMR** (DMSO-d_6) δ 2.05 (s, 3H, CH_3), 3.09 (t, 2H, J = 5.0, CH_2N(Ph)CH_2), 3.16 (t, 2H, J = 5.0, CH_2N(Ph)CH_2), 3.58–3.60 (m, 4H, CH_2N(COCH_3)CH_2), 7.01 (d, 2H, J = 8.5, 2 × Ph-H), 7.18–7.33 (m, 1H, indazolyl-H), 7.46–7.60 (m, 3H, indazolyl-H & 2 × Ph-H), 7.68 (d, 1H, J = 8.5, indazolyl-H), 8.84 (s, 1H, pyrimidinyl-H), 10.22 (s, 1H, indazolyl-H), 13.99 (s, 1H, indazolyl-NH) (one proton signal (pyrimidinyl–NH–Ph) not observed). **^{13}C NMR** (DMSO-d_6) δ 21.3, 40.7, 45.5, 48.6, 48.9, 49.3, 110.9, 116.3, 117.9, 121.6, 122.0, 122.6, 123.6, 127.0, 140.1, 141.2, 159.9,

160.9, 164.1, 168.3 (four carbon signals overlapping or obscured). **HRMS** (ESI-TOF) *m/z* 439.1980 $[M+H]^+$; calcd. for $C_{24}H_{23}N_8O^+$ 439.1989 $[M+H]^+$. **Anal. RP-HPLC**: t_R = 19.40 min, purity >95% (method A); t_R = 15.21 min, purity > 95% (method B).

1-(4-(3-((4-(1*H*-Indazol-3-yl)pyrimidin-2-yl)amino)phenyl)-1,4-diazepan-1-yl)ethan-1-one (12s)

Guanidine **11c** (300 mg, 1.08 mmol) and enaminone **8j** (110 mg, 510 μmol) were coupled using general synthetic procedure E. The residue was purified by FlashMaster Personal$^+$ chromatography (silica gel, DCM ramping to DCM:CH_3OH = 96:4 + 0.2% NH_3 (32% in H_2O)) and washed with CH_3OH (10 mL) to give **12s** as a white solid (42 mg, 19%). **m.p.** 189–191 °C. **^{1}H NMR** (DMSO-d_6) (**12s** exists as two rotamers in approximately 1:1 ratio.) δ 1.79–1.83 (m, 1H, $CH_2CH_2CH_2$ of one rotamer), 1.87 (s, 1.5H, CH_3 of one rotamer), 1.88–1.92 (m, 1H, $CH_2CH_2CH_2$ of the other rotamer), 1.99 (s, 1.5H, CH_3 of the other rotamer), 3.31 (t, 2H, *J* 5.5), 3.50 (t, 2H, *J* 5.5), 3.54 (t, 1H, *J* 5.5), 3.58–3.63 (m, 2H), 3.66 (t, 1H, *J* 5.0) (total 8H, $CH_2N(COCH_3)CH_2$ & $CH_2N(Ph)CH_2$), 6.42 (d, 1H, *J* 8.0, Ph-H), 7.11 (t, 1H, *J* 8.0, Ph-H), 7.15 (s, 1H, Ph-H), 7.25 (d, 1H, *J* 8.0, Ph-H), 7.28 (ddd, 1H, *J* 7.5 & 6.5 & 0.5, indazolyl-H), 7.44 (t, 1H, *J* 7.5, indazolyl-H), 7.48 (d, 1H, *J* 5.0, pyrimidinyl-H), 7.63 (d, 1H, *J* 8.5, indazolyl-H), 8.50 (d, 1H, *J* 5.5, pyrimidinyl-H), 8.73 (d, 1H, *J* 7.5, indazolyl-H), 9.40 (s, 1H, pyrimidinyl–NH–Ph), 11.98 (s, 1H, indazolyl-NH). **^{13}C NMR** (DMSO-d_6) δ 21.0, 21.3 (one carbon), 24.0, 25.8 (one carbon), 43.9, 44.5, 46.9, 47.0, 47.2, 48.2, 49.1, 49.7 (four carbons), 89.2, 102.8, 102.9 (one carbon), 105.6, 105.7 (one carbon), 107.3, 107.6 (one carbon), 110.6, 121.1, 121.8, 123.2, 126.6, 129.2, 141.2, 141.5, 141.6, 141.7 (one carbon), 147.3, 147.6 (one carbon), 158.0, 160.3, 160.7, 169.0, 169.3 (one carbon). **HRMS** (ESI-TOF) *m/z* 428.2201 $[M+H]^+$; calcd. for $C_{24}H_{26}N_7O^+$ 428.2193 $[M+H]^+$. **Anal. RP-HPLC**: t_R = 19.61 min, purity >99% (method A); t_R = 14.77 min, purity > 99% (method B).

4.3. Kinase assays

The percentages of residual kinase activity of **12b** in the panel screen and the half maximal inhibitory concentration (IC_{50}) values of the reported compounds against each kinase were mostly determined by Reaction Biology Corporation (Malvern, PA, USA, www.reactionbiology.com). In brief, specific kinase-substrate pairs together with the required cofactors were prepared in freshly-made base reaction buffer (20 mM HEPES pH 7.5, 10 mM $MgCl_2$, 1 mM EGTA, 0.02% Brij 35, 0.02 mg/mL BSA, 0.1 mM Na_3VO_4, 2 mM DTT, 1% DMSO). Compounds in DMSO were delivered into the reaction mixture by Acoustic technology (Echo550; nanoliter range). The reaction mixtures were incubated for 20 min at room temperature and ^{33}P-ATP with a specific activity of 10 μCi/μL was added to initiate the reaction. Reactions were carried out at room temperature for 2 h, followed by spotting of the reactions onto P81 ion exchange filter papers. Phosphoric acid (0.75%) was used to wash unbound phosphate from the filters. The percentages of remaining kinase activity in tested samples were measured by comparison to vehicle (DMSO) reactions after subtraction of the background derived from the control reactions containing inactive kinase. IC_{50} values and curve fits were obtained using Prism (GraphPad Software, La Jolla, California, USA). K_i values were calculated using the Cheng-Prusoff equation: $K_i = IC_{50}/(1 + ([ATP]/K_m(ATP)))$, where [ATP] is K_m(ATP) according to the Reaction Biology Corporation binning structure.

Some of the CDK and FLT3 kinase assays were performed in-house. The CDK kinase activity assays were validated and performed using an ADP-Glo™ assay kit (Promega Corporation, Madison, WI, USA). Compounds were prepared as 2 mM stocks in 100% DMSO and stored at −20 °C. For determination of % inhibition and IC_{50}, the assays were conducted using 384-well, low volume, non-binding white polystyrene plates. Compounds were added either at single concentration of 1 μM for initial evaluation or at 8–10 concentrations (1:3 serial dilutions from 3 μM) for IC_{50} determination in a total assay volume of 4 μL with a final DMSO concentration of 0.5% in all wells. Optimised concentration of each kinase (CDK1/cyclin B: 1 nM, CDK2/cyclin E1: 10 nM, and CDK7/cyclin H/MAT1: 40 nM) was then incubated with tested compounds, their substrates (histone 1 protein for CDK1/cyclin B and CDK2/cyclin E1 and a peptide based upon the c-terminal tail of RNA polymerase II, H-YSPTSPSYSPTSPSYSPTSPSKKKK-OH for CDK7/cyclin H/MAT1) and K_m (ATP) for each kinase. The reaction was performed in kinase reaction buffer; 40 mM Tris base (pH 7.5), 20 mM $MgCl_2$, 50 μM DTT and 0.1 mg/mL BSA. Positive and negative controls were performed in 0.5% DMSO in the presence and absence of each kinase. The assay plate was then incubated at room temperature for an optimised time period for each kinase, generally 60–120 min. Following incubation, 4 μL of ADP-Glo reagent was added to each well and incubated for 40 min in the dark at room temperature. Then 8 μL of detection reagent was added to all the wells and then further incubated for 40 min in the dark. Luminescence was measured with an EnVision Multilabel plate reader (PerkinElmer, Buckinghamshire, UK) with an integration time of 1 s per well. The luminescence thus generated correlates with kinase activity. The IC_{50} values were derived by fitting a sigmoidal dose-response curve using non-linear regression 4-parameter logistic fits (variable slope) by GraphPad Prism software 8.3.0 (La Jolla, CA, USA). For FLT3 kinase assays, compounds were used with 1:3 serial dilutions for 10 concentrations (from 10 to 0.0005 μM). The kinase reactions were performed with the kinase reaction buffer (40 nM Tris base pH 7.5, 20 mM $MgCl_2$, 50 μM DTT, 0.1 mg/mL BSA), the poly(Glu, Tyr) (the ratio of Glu/Tyr = 4:1) peptide substrate, K_m ATP (FLT3-WT: 200 μM; FLT3-ITD: 100 μM) and an FLT3 kinase (FLT3-WT: 20 nM; FLT3-ITD: 20 nM) in a total assay volume of 5 μL. The kinase reactions were run for an optimised time period (FLT3-WT: 120 min; FLT3-ITD: 80 min) at room temperature and stopped by adding 5 μL of ADP Glo reagent. After incubation at room temperature in the dark for 40 min, 10 μL of kinase detection reagent was added to each well and incubated for 30–40 min. Luminescence was measured using the EnVision multilabel plate reader with an integration time of 1 s per well. Positive and negative controls were performed in 0.5% DMSO in the presence and absence of each FLT3 kinase, respectively.

4.4. Cell culture

MV4-11 cells were kindly provided by Professor Richard D'Andrea from University of South Australia. All other cell lines were purchased from the American Tissue Culture Collection (ATCC) (Manassas, VA, USA). The cell lines were maintained following ATCC recommendation in Roswell Park Memorial Institute (RPMI)-1640, Dulbecco's Modified Eagle's Medium (DMEM) or Minimum Essential Medium (MEM) with 10% foetal bovine serum (FBS) (Sigma-Aldrich, Castle Hill, NSW, Australia). All the cell lines were cultured at 37 °C in a humidified incubator in the presence of 5% CO_2 atmosphere.

4.5. Cell viability assays

Resazurin assays were performed with each of leukaemic cell lines (*i.e.*, MV4-11, MOLM-13, NB4, THP1, U937, Jurkat and K562) according to manufacturers' instructions. Cells were seeded at 5×10^3 cells/well onto 96-well cell culture plates and incubated at 37 °C, 5% CO_2 for 24 h. Tested compounds were diluted from a 10 mM stock solution to prepare a five-fold dilution series in 100 μL of cell medium, added to cells (in triplicate), and incubated at 37 °C,

5% CO_2 for 24 or 72 h. Resazurin (Sigma-Aldrich, Castle Hill, NSW, Australia) was made up as a stock of 0.1 mg/mL in cell medium, and the solution was filter-sterilised. Resazurin solution was added at 20 μL/well and incubated in the dark at 37 °C, 5% CO_2 for 4 h. The plate was left at room temperature for 10–15 min, and the fluorescent product quantified using the EnVision multi-label plate reader with a 570 nm (excitation)/585 nm (emission) filter set. The drug-treated samples were normalised to a vehicle control (100% DMSO). Compound concentrations required to inhibit 50% of cell growth (*i.e.*, GI_{50} values) were calculated using non-linear regression analysis (GraphPad Prism v.7, La Jolla, CA, USA).

4.6. Detection of apoptosis

MV4-11 and U937 cells were plated at a cell density of 3×10^5 and cultured in 3 mL of medium per well in a six-well plate for 24 h. The cells were subsequently treated with the vehicle control (100% DMSO) or each compound at concentrations of 1 ×, 5 ×, 10 × and 20 × GI_{50} (GI_{50} refers to the 24 h value of MV4-11 cells for each compound) for 24 and/or 48 h. The media containing the cells were transferred to FACS tubes, centrifuged for 5 min at 300 *g* and re-suspended in 1 mL of warm 1 × PBS to wash cells. The cells were counted using an automated cell counter (Bio-Rad) using 10 μL of the cell suspension, and subsequently diluted to 2×10^5 cells/mL with 1 mL PBS in a new FACS tube. Lastly, the cells were centrifuged for an additional 5 min at 300 *g*, re-suspended in 1 mL of ice-cold 1 × PBS, re-centrifuged at 300 *g* for 5 min, re-suspended in a solution of 1 × binding buffer (100 μL), annexin V (3 μL) and PI (3 μL), and incubated at room temperature for 15 min. A final 200 μL of 1 × binding buffer was added to the cell samples, and they were analysed by flow cytometry using a CytoFlex (Beckman Coulter) operating machine. Four control samples included in all flow cytometry experiments are (1) unstained cells, (2) cells stained with annexin V (no PI), (3) cells stained with PI (no annexin V) and (4) cells stained with both annexin V and PI (used as no treatment control). Statistical analysis was performed using GraphPad one-way ANOVA analysis with Tukey's post-hoc test, and statistical significance was defined as a *p*-value of <0.05 (*), <0.01 (**), <0.001 (***) and <0.0001 (****) (GraphPad Prism v.7, La Jolla, CA, USA).

4.7. Western blots

Antibodies raised against phospho-STAT5 (Tyr 694; C11C5), phospho-AKT (Ser473), phospho-p44/42 MAPK (ERK 1/2) (Thr202/Tyr204), phospho-eIF4E (Ser209), phospho-S6RP (Ser235/Ser236), full-length and cleaved PARP and caspase 3, Mcl-1 and β-actin were purchased from Cell Signaling Technology (Beverley, MA). A secondary anti-rabbit HRP antibody was purchased from DAKO (Mulgrave, VIC). The iBolt blotting system was purchased from Thermo-Scientific (Waltham, MA)and an ECL-western blotting reagents were purchased from GE Healthcare (Amersham, United Kingdom).

MV4-11 or U937 cells were plated in 10 cm petri dishes a cell density of 1.5×10^6 and cultured for 24 h for protein lysate preparation. Subsequently, the cells were treated for 6 and/or 24 h with the vehicle control (100% DMSO) or each compound at concentrations of 1 ×, 10 × and 20 × GI_{50} (GI_{50} refers to the 24 h value of MV4-11 cells for each compound). Cells were centrifuged at 300 *g* for 5 min, and further re-suspended in cold 1 × phosphate lysis buffer plus protease inhibitors. A Bio-Rad protein assay was performed to determine the protein concentration and 20 μg of total protein was separated on pre-cast SDS-polyacrylamide gels and transferred to nitrocellulose membranes using the iBolt blotting system. The membranes were blocked in 10% skim-milk powder plus 1 × TBST and further probed with primary antibodies at 4 °C to detect the steady-state protein levels of phosphorylated and/or total STAT5, AKT, ERK, S6RP, eIF4E, full-length and cleaved PARP and caspase-3, Mcl-1 and β-actin according to manufacturers' specifications. The secondary anti-rabbit HRP antibody was further used to probe the membranes for 1 h at room temperature. Subsequently, the ECL-reagent was added to the membranes and image analysis using a Bio-Rad ChemiDoc™ MP imager was performed for band detection and image production.

Declaration of competing interest

The authors declare that they have no known competing financial interests or personal relationships that could have appeared to influence the work reported in this paper.

Acknowledgements

This work was supported by The Financial Markets Foundation for Children (Project 2019-112) to S.W. and Channel 7 Children's Research Foundation of South Australia (project ID 19/10674521) to M.Y.

Appendix A. Supplementary data

Supplementary data to this article can be found online at https://doi.org/10.1016/j.ejmech.2021.113215.

References

[1] M.-A. Hospital, A.S. Green, T.T. Maciel, I.C. Moura, A.Y. Leung, D. Bouscary, J. Tamburini, FLT3 inhibitors: clinical potential in acute myeloid leukemia, OncoTargets Ther. 10 (2017) 607.
[2] S.A. Wander, M.J. Levis, A.T. Fathi, The evolving role of FLT3 inhibitors in acute myeloid leukemia: quizartinib and beyond, Therapeut. Adv. Hematol. 5 (3) (2014) 65–77.
[3] A. Leung, C. Man, Y. Kwong, FLT3 inhibition: a moving and evolving target in acute myeloid leukaemia, Leukemia 27 (2) (2013) 260–268.
[4] M.M. Gallogly, A.E. Perl, H.M. Lazarus, Midostaurin and emerging FLT3 inhibitors for the treatment of adults with newly diagnosed acute myeloid leukemia with the FLT3 mutation, Expert Rev. Precis. Med. Drug Dev. 2 (6) (2017) 307–320.
[5] H. Döhner, D.J. Weisdorf, C.D. Bloomfield, Acute myeloid leukemia, N. Engl. J. Med. 373 (12) (2015) 1136–1152.
[6] K.A. Minson, C.C. Smith, D. DeRyckere, C. Libbrecht, A.B. Lee-Sherick, M.G. Huey, E.A. Lasater, G.D. Kirkpatrick, M.A. Stashko, W. Zhang, The MERTK/FLT3 inhibitor MRX-2843 overcomes resistance-conferring FLT3 mutations in acute myeloid leukemia, JCI Insight 1 (3) (2016), e85630.
[7] C.E. Carow, M. Levenstein, S.H. Kaufmann, J. Chen, S. Amin, P. Rockwell, L. Witte, M.J. Borowitz, C.I. Civin, D. Small, Expression of the hematopoietic growth factor receptor FLT3 (STK-1/Flk2) in human leukemias, Blood 87 (3) (1996) 1089–1096.
[8] O. Rosnet, C. Schiff, M.J. Pebusque, S. Marchetto, C. Tonnelle, Y. Toiron, F. Birg, D. Birnbaum, Human Flt3/Flk2 gene: cDNA cloning and expression in hematopoietic cells, Blood 82 (4) (1993) 1110–1119.
[9] S.D. Lyman, S.E.W. Jacobsen, c-Kit ligand and flt3 ligand: stem/progenitor cell factors with overlapping yet distinct activities, Blood 91 (4) (1998) 1101–1134.
[10] S. Meshinchi, F.R. Appelbaum, Structural and functional alterations of FLT3 in acute myeloid leukemia, Clin. Canc. Res. 15 (13) (2009) 4263–4269.
[11] K. Verstraete, G. Vandriessche, M. Januar, J. Elegheert, A.V. Shkumatov, A. Desfosses, K. Van Craenenbroeck, D.I. Svergun, I. Gutsche, B. Vergauwen, S.N. Savvides, Structural insights into the extracellular assembly of the hematopoietic Flt3 signaling complex, Blood 118 (1) (2011) 60–68.
[12] S. Knapper, FLT3 inhibition in acute myeloid leukaemia, Br. J. Haematol. 138 (6) (2007) 687–699.
[13] D.L. Stirewalt, J.P. Radich, The role of FLT3 in haematopoietic malignancies, Nat. Rev. Canc. 3 (9) (2003) 650–665.
[14] T.L. Gu, J. Nardone, Y. Wang, M. Loriaux, J. Villen, S. Beausoleil, M. Tucker, J. Kornhauser, J.M. Ren, J. MacNeill, S.P. Gygi, B.J. Druker, M.C. Heinrich, J. Rush, R.D. Polakiewicz, Survey of activated FLT3 signaling in leukemia, PloS One 6 (4) (2011), e19169.
[15] J.A. McCubrey, L.S. Steelman, S.L. Abrams, F.E. Bertrand, D.E. Ludwig, J. Basecke, M. Libra, F. Stivala, M. Milella, A. Tafuri, P. Lunghi, A. Bonati, A.M. Martelli, Targeting survival cascades induced by activation of Ras/Raf/MEK/ERK, PI3K/

PTEN/Akt/mTOR and Jak/STAT pathways for effective leukemia therapy, Leukemia 22 (4) (2008) 708–722.
[16] G. Marcucci, T. Haferlach, H. Dohner, Molecular genetics of adult acute myeloid leukemia: prognostic and therapeutic implications, J. Clin. Oncol. 29 (5) (2011) 475–486.
[17] A.T. Fathi, Y.B. Chen, The role of FLT3 inhibitors in the treatment of FLT3-mutated acute myeloid leukemia, Eur. J. Haematol. 98 (4) (2017) 330–336.
[18] E. Weisberg, C. Boulton, L.M. Kelly, P. Manley, D. Fabbro, T. Meyer, D.G. Gilliland, J.D. Griffin, Inhibition of mutant FLT3 receptors in leukemia cells by the small molecule tyrosine kinase inhibitor PKC412, Canc. Cell 1 (5) (2002) 433–443.
[19] D.G. Gilliland, J.D. Griffin, The roles of FLT3 in hematopoiesis and leukemia, Blood 100 (5) (2002) 1532–1542.
[20] K. Ozeki, H. Kiyoi, Y. Hirose, M. Iwai, M. Ninomiya, Y. Kodera, S. Miyawaki, K. Kuriyama, C. Shimazaki, H. Akiyama, Biologic and clinical significance of the FLT3 transcript level in acute myeloid leukemia, Blood 103 (5) (2004) 1901–1908.
[21] M. Levis, Midostaurin approved for FLT3-mutated AML, Blood 129 (26) (2017) 3403–3406.
[22] M.R. Grunwald, M.J. Levis, FLT3 inhibitors for acute myeloid leukemia: a review of their efficacy and mechanisms of resistance, Int. J. Hematol. 97 (6) (2013) 683–694.
[23] M.B. Leick, M.J. Levis, The future of targeting FLT3 activation in AML, Curr. Hematol. Malig. Rep. 12 (3) (2017) 153–167.
[24] D. Pastore, FLT3 inhibitors in acute myeloid leukemia, DCTH 4 (1) (2016) 14–21.
[25] N. Pemmaraju, H. Kantarjian, M. Andreeff, J. Cortes, F. Ravandi, Investigational FMS-like tyrosine kinase 3 inhibitors in treatment of acute myeloid leukemia, Expet Opin. Invest. Drugs 23 (7) (2014) 943–954.
[26] S. Wang, C. Meades, G. Wood, A. Osnowski, S. Anderson, R. Yuill, M. Thomas, M. Mezna, W. Jackson, C. Midgley, 2-Anilino-4-(thiazol-5-yl) pyrimidine CDK inhibitors: synthesis, SAR analysis, X-ray crystallography, and biological activity, J. Med. Chem. 47 (7) (2004) 1662–1675.
[27] S. Wang, G. Griffiths, C.A. Midgley, A.L. Barnett, M. Cooper, J. Grabarek, L. Ingram, W. Jackson, G. Kontopidis, S.J. McClue, Discovery and characterization of 2-anilino-4-(thiazol-5-yl) pyrimidine transcriptional CDK inhibitors as anticancer agents, Chem. Biol. 17 (10) (2010) 1111–1121.
[28] S. Diab, A.M. Abdelaziz, P. Li, T. Teo, S.K.C. Basnet, B. Noll, M.H. Rahaman, J.F. Lu, J.Q. Hou, M.F. Yu, B.T. Le, H. Albrecht, R.W. Milne, S.D. Wang, Dual inhibition of Mnk2 and FLT3 for potential treatment of acute myeloid leukaemia, Eur. J. Med. Chem. 139 (2017) 762–772.
[29] S. Tadesse, M. Yu, L.B. Mekonnen, F. Lam, S. Islam, K. Tomusange, M.H. Rahaman, B. Noll, S.K. Basnet, T. Teo, Highly potent, selective, and orally bioavailable 4-thiazol-N-(pyridin-2-yl) pyrimidin-2-amine cyclin-dependent kinases 4 and 6 inhibitors as anticancer drug candidates: design, synthesis, and evaluation, J. Med. Chem. 60 (5) (2017) 1892–1915.
[30] H. Shao, S. Shi, S. Huang, A.J. Hole, A.Y. Abbas, S. Baumli, X. Liu, F. Lam, D.W. Foley, P.M. Fischer, Substituted 4-(Thiazol-5-yl)-2-(phenylamino) pyrimidines are highly active CDK9 inhibitors: synthesis, X-ray crystal structures, structure–activity relationship, and anticancer activities, J. Med. Chem. 56 (3) (2013) 640–659.
[31] P.M. Lukasik, S. Elabar, F. Lam, H. Shao, X. Liu, A.Y. Abbas, S. Wang, Synthesis and biological evaluation of imidazo [4, 5-b] pyridine and 4-heteroaryl-pyrimidine derivatives as anti-cancer agents, Eur. J. Med. Chem. 57 (2012) 311–322.
[32] H. Shao, S. Shi, D.W. Foley, F. Lam, A.Y. Abbas, X. Liu, S. Huang, X. Jiang, N. Baharin, P.M. Fischer, Synthesis, structure–activity relationship and biological evaluation of 2, 4, 5-trisubstituted pyrimidine CDK inhibitors as potential anti-tumour agents, Eur. J. Med. Chem. 70 (2013) 447–455.
[33] O.P. Van Linden, A.J. Kooistra, R. Leurs, I.J. De Esch, C. De Graaf, KLIFS: a knowledge-based structural database to navigate kinase–ligand interaction space, J. Med. Chem. 57 (2) (2013) 249–277.
[34] P.P. Zarrinkar, R.N. Gunawardane, M.D. Cramer, M.F. Gardner, D. Brigham, B. Belli, M.W. Karaman, K.W. Pratz, G. Pallares, Q. Chao, AC220 is a uniquely potent and selective inhibitor of FLT3 for the treatment of acute myeloid leukemia (AML), Blood 114 (14) (2009) 2984–2992.
[35] T. Odgerel, J. Kikuchi, T. Wada, R. Shimizu, K. Futaki, Y. Kano, Y. Furukawa, The FLT3 inhibitor PKC412 exerts differential cell cycle effects on leukemic cells depending on the presence of FLT3 mutations, Oncogene 27 (22) (2008) 3102–3110.
[36] H. Quentmeier, J. Reinhardt, M. Zaborski, H. Drexler, FLT3 mutations in acute myeloid leukemia cell lines, Leukemia 17 (1) (2003) 120–124.
[37] B. Xu, Y. Zhao, X. Wang, P. Gong, W. Ge, MZH29 is a novel potent inhibitor that overcomes drug resistance FLT3 mutations in acute myeloid leukemia, Leukemia 31 (4) (2017) 913–921.
[38] A.S. Moore, A. Faisal, D.G. De Castro, V. Bavetsias, C. Sun, B. Atrash, M. Valenti, A. de Haven Brandon, S. Avery, D. Mair, Selective FLT3 inhibition of FLT3-ITD+ acute myeloid leukaemia resulting in secondary D835Y mutation: a model for emerging clinical resistance patterns, Leukemia 26 (7) (2012) 1462–1470.
[39] C.C. Smith, K. Lin, A. Stecula, A. Sali, N.P. Shah, FLT3 D835 mutations confer differential resistance to type II FLT3 inhibitors, Leukemia 29 (12) (2015), 23902392.
[40] R. Dienstmann, J. Rodon, V. Serra, J. Tabernero, Picking the point of inhibition: a comparative review of PI3K/AKT/mTOR pathway inhibitors, Mol. Canc. Therapeut. 13 (5) (2014) 1021–1031.
[41] S. Park, N. Chapuis, J. Tamburini, V. Bardet, P. Cornillet-Lefebvre, L. Willems, A. Green, P. Mayeux, C. Lacombe, D. Bouscary, Role of the PI3K/AKT and mTOR signaling pathways in acute myeloid leukemia, Haematol-Hematol. J. 95 (5) (2010) 819–828.
[42] J.K. Altman, A. Sassano, L.C. Platanias, Targeting mTOR for the treatment of AML. New agents and new directions, Oncotarget 2 (6) (2011) 510–517.
[43] A. Nogami, G. Oshikawa, K. Okada, S. Fukutake, Y. Umezawa, T. Nagao, T. Kurosu, O. Miura, FLT3-ITD confers resistance to the PI3K/Akt pathway inhibitors by protecting the mTOR/4EBP1/Mcl-1 pathway through STAT5 activation in acute myeloid leukemia, Oncotarget 6 (11) (2015) 9189–9205.